Experimental and Numerical Analyses of Torque Properties of Rotary Elastomer Particle Damper

（回転型エラストマー粒状体ダンパーのトルク特性
に関する実験および数値解析）

A Thesis Submitted to Nagoya institute of Technology
in Partial Fulfillment of the Requirement for the
Ph.D. Degree

ALLAH RAKHIO

Supervised by: Prof. Yasushi Ido

Department of Electrical and Mechanical Engineering,
Nagoya Institute of Technology

Table of Contents

1. Introduction

1.1 Vibration and damping

Continous stresses and strains due to unwanted vibrations are one of the major sources of failures of mechanical systems and structures. Mechanical systems and structures (i.e., buildings, bridges, automobiles, and parts of automobiles) can break earlier than expected due to unwanted vibrations. Sudden breaking of any mechanical system and structure can be dangerous to human life. Vibration can also cause noise and disturbance, which can also affect human health. While designing mechanical systems and structures, attention must be given to the decrease the vibrations. To some extent, the vibration can be controlled by the dynamic balancing of the moving parts, but after a certain limit due to the motion of components further reduction is not possible by balancing. In this situation, the damping source is attached to the mechanical systems and structures to reduce vibration.

The damping of any mechanical system and structure can be divided into passive damping, active damping, hybrid damping, and semi-active damping [1]. Damping can be active damping and passive damping. Active damping is achieved by exerting a counterforce or moment in a controlled manner. For passive damping, the damping is produced without an external source of energy. The active damping is produced by applying external energy to the damping unit. In the case of hybrid damping, the combination of passive and active damping is provided to the mechanical system and structure. In semi-active damping, the damping can be adjusted according to the reaction of mechanical systems.

A practical example is semi-active suspensions in the latest automobiles using viscous fluid as a vibration suppression medium. There are different types and methods for semi-active suspension system. For the semiactive suspension system, magnetorheological (MR) fluids are also used. MR fluid is a kind of fluid that can change from a liquid state to a semi-solid state when subjected to a magnetic field [2]. One of the main problems with conventional dampers is that the performance is sensitive to temperature [3, 4]. The suitable temperature range for conventional dampers

is less than 250 degrees Celsius [4]; however, a high-temperature range is required [5]. The second problem with conventional dampers is oil leakage. In recent years, researchers have turned their focus extensively on particle dampers. Particle dampers can be used in harsh environments where conventional dampers are inefficient [6, 7]. Compared to a conventional oil damper, a particle damper has a wider control frequency band [8].

Particle dampers use different techniques than oil dampers to control the vibration from mechanical systems and structures. The damping devices are categorized as friction dampers (FDs), tuned mass dampers (TMDs), and viscous fluid dampers (VFDs), and isolators [9]. Particle damper is the device in which particles move freely in a cavity to produce a damping effect. In this dissertation, we are focusing on the damping characteristics of particle dampers.

1.2 Brief overview of particle dampers

Particle dampers consist of container-filled particles made from different materials, i.e., glass, lead, tungsten, elastomers, etc. [10-12]. The damper dissipates energy due to collision and friction between the particle-particle and particle-wall of the damper [13]. Particle dampers have a simple structure, and they have a wide range of practical applications, such as, civil structure, mechanical structures, and vehicles.

The concept of particle damping dates back to 1937, when the turbine blade's vibration control impact damping concept was first proposed by Paget [14]. The damping technique consisted of a single particle. Although the concept was unique for vibration attenuation, the main problem with the damper was loud noise due to collision. In 1945, Lieber and Jansen proposed a vibration control technique for mechanical systems [15]. In their research, the frequency was kept fixed, and a large ratio of damper mass to machine mass was feasible.

1.2.1 Types of particle dampers

Based on the number of particles, the particle dampers can be divided into four main types: impact damper [15], multi-unit impact damper [16], particle damper [17], and multi-unit particle damper [18]. Impact damper consisted of a single particle in a single cavity. Multi-unit impact damper consisted of more than one cavity with single

particle in each cavity. In particle dampers several particles are used in single cavity. Multi-unit impact damper consisted of more than one cavity with several particles in each cavity. Masri performed experiments and simulations to verify that multi-unit impact dampers are more effective than single-unit impact dampers [19]. The development of these four basic types evolved into several other types and parameter studies in particle damping.

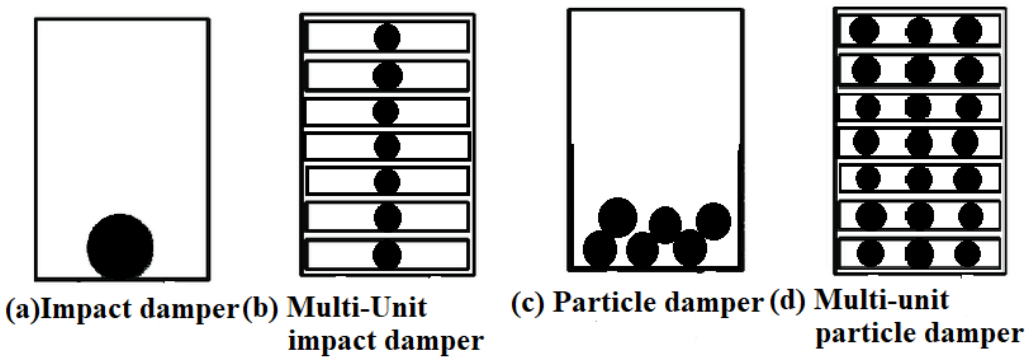

Fig.1.1 Basic types of particle dampers [20]

In 1991, Panossian proposed a non-obstructive particle damper [21]. He used small cavities at different locations inside the mechanical structure. Cavities were filled with particles made from different materials (steel, tungsten powder, nickel powder, etc.). A decrease in vibrations of the mechanical structure was observed in his results. In 2010, Hayashi and Ido proposed a novel particle damper that consisted of glass particles as a damping medium. Their design consisted of a piston with linear motion, as shown in Fig 1.2 [22]. They concluded that the packing fraction, vibration frequency, and particle size significantly affect particle damper's damping performance. Their study further extended the type of particle dampers into piston-based particle dampers. Later, Ido et al. investigated the damping properties of a damper using steel particle assemblage [23]. It was noted that the damping force of low frequency is quite different from that of the relatively high frequency of forced vibration. An increase in the damper force is observed with an increase in the length of the inner area. Hanai et al. verified the experimental results and investigated the behavior of steel particles in a linear damper using the discrete element method [24]. The results showed that the damping force is mainly affected by the elastic and frictional forces of particles.

Kawamoto et al. investigated the effect of gravity on the steel particles used inside a linear damper [25]. To reduce the effect of gravity, two permanent magnets with opposite poles were attached to the sides of the damper. Binoy et al. [26] proposed a semi-active piston-based particle damper. In his design, the external magnetic field is provided to the magnetic particles inside the damper. Gharib et al. proposed a linear particle chain type damper based on small balls between large size balls inside a damper, as shown in Fig.1.3 [27]. Several studies have been conducted on particle impact dampers. Marhadi, et al. proposed a particle impact damper for beam [12], the effect of packing fraction was investigated. They suggested that the size and the number of particles are independent parameters and should be considered while designing particle impact dampers. Liu, et al. studied the vibration control of structures using particle impact dampers [11]; they found that the disk cavity's ratio of thickness to diameter plays a significant role in increasing the damping characteristics.

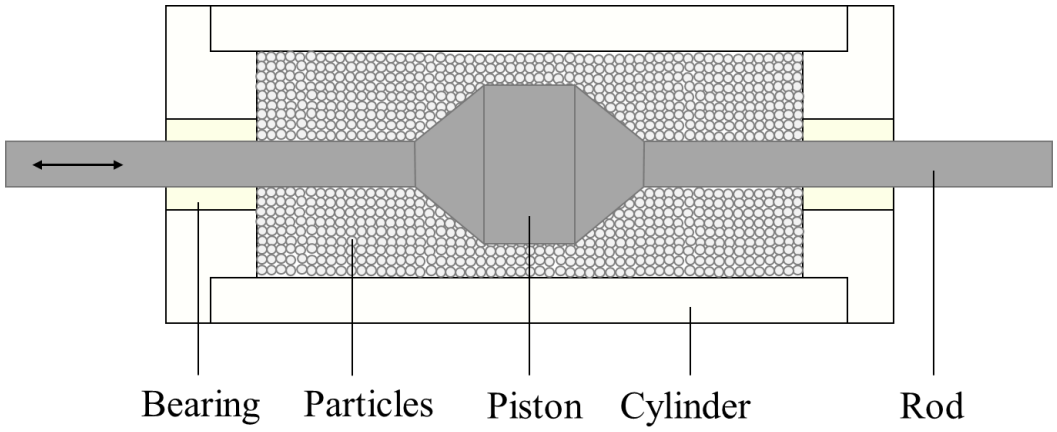

Fig.1.2 Piston-based particle damper [22]

Most of the published work is based on particle impact dampers, while limited articles have been found on piston-based particle dampers. Kawamoto et al. proposed to use elastomer particles containing micron size silicon particles in their piston-based particle damper [28]. Morishita et al. proposed a piston-based elastomer particle damper, and they used a double rod type particle damper [10]. In their paper, they concluded that an increase of packing fraction, frequency, and stroke of the piston increases the damper

force. Toyouchi et al. introduced a linear type dual-chamber single-rod-type particle damper [29]. They showed that the influence of the vibration frequency on the damper force is small with respect to the influence of the packing fraction on the damper force. Kishan et al. proposed a rotary elastomer particle damper, whose torque depends on the rotor angle [30]. In their research, they used a rotor inside the damper. A rotating rod is used instead of a piston. As for as author's knowledge, no more articles have been found on the damper torque properties of a rotary elastomer particle damper.

Based on the literature review, there are two types of dampers used in the particle-based vibration control system. One is a particle impact damper, and the other is a piston and rotor-based particle damper. Particle impact dampers consist of a closed cavity with particles inside it. In piston and rotor-based particle dampers, a moving rod or rotor is used inside the container of the damper. The piston-based particle damper is a linear damper consisting of a rod, and a rotary particle damper consists of a rotating shaft. Fig 1.4 shows the particle damper categorization.

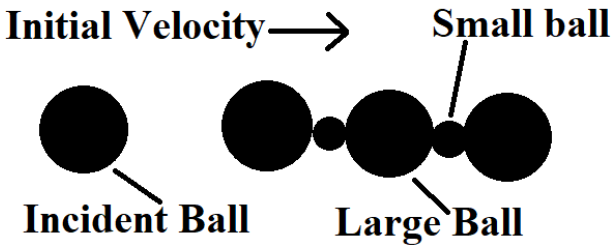

Fig.1.3 Gahrib's damper with small and large balls [27]

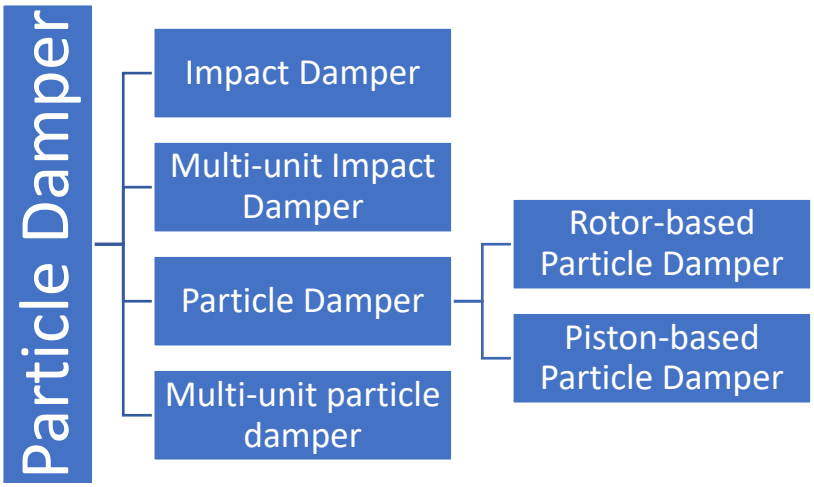

Fig.1.4 Particle damper categorization

1.2.2 Type and size of particles used for particle damping

Different researchers have studied different types of materials as particles inside the damper. Some researchers investigated traditional materials with different techniques, and some of them tried traditional techniques with different types of particles. The main purpose of investigating particles made of different materials was to reduce the noise, impact forces, and increase plastic deformation, thus increasing the damping characteristics of particle dampers. A particle damper with the inner wall made of rubber was investigated by Li [31]. Based on experimental results, it was proved that due to the usage of rubber in the inner wall, a significant amount of reduction in impact forces and noise due to the collision was observed. The fine particle impact damper idea was put forward by Du [32]. He used fine particles as a damping medium to absorb the vibration of the mechanical structure. Darabi et al. used polymeric particles [33]. They proposed that after the convection region, the damping properties of the damper are irrespective of the type of materials. Particle dampers consisting of elastomer particles were put forward by Bustamante et al. [34]. A particle damper with soft hollow particles was proposed by Michon et al. [35]. They concluded that soft hollow particles are suitable for damping when the frequency is higher.

Hamzeh et al. conducted a detailed investigation of the shape of the particles [36]. They reported that spherical shape is the most favorable shape to be used in particle impact dampers. Research on the effect of the particles packing fraction and size of metallic particles was conducted by Kachare and Bimlesh [37]; they used 1 mm, 2 mm, and 3 mm diameter spherical particles made of copper. They concluded that 1 mm diameter-sized particle showed the highest performance among them.

Elastomer particles are used in this study due to the high excitation intensity of elastomer particles. They produce less noise due to collisions and they are lighter and cheaper than metallic particles.

1.3 Damping mechanism of particle dampers

The vibration control of particle dampers is due to friction and collisions between particles and between particles and walls of the damper. Friction and collision between particles result in energy dissipation which results in the generation of damping forces. Different researchers argued on the damping mechanism of particle dampers and

proposed different theories of damping mechanism. Kervin proposed that damping takes place due to the friction between particle-particle, deformation of particles, and resonance of material of particles [38]. Popplewell suggested that energy dissipation occurs due to the momentum exchange of particles when they collide with each other and the walls of the damper [39]. A study on the energy dissipation of particles in a particle damper based on the discrete element method (DEM) was conducted by Wong, et al. [40]. He concluded that friction plays a vital role in the vibration control mechanism of particle dampers. Chen, et al. [41] put forward the concept that energy dissipation occurs in a particle damper due to thermal energy and potential energy. Based on the DEM simulations proved that the properties of the particles used inside the particle damper have little influence on its damping properties if the clearance inside the damper is changed accordingly [42]. Sanchez, et al. [43] concluded that the welding of individual particles can reduce the particle damper's performance.

1.4 Numerical simulations in the field of particle damping

The DEM is mostly used numerical simulation method for particle behavior analysis. DEM was first proposed by Cundall [44] as a granular particle flow analysis technique. The DEM analyzes the behavior of particles based on contact laws and equations of motion. DEM is a simple method to analyze particle behavior, but it is a lengthy method, especially when large numbers of particles are analyzed [45]. Considering the long duration of DEM simulation, different scholars put forward some simplified DEM techniques to analyze the behavior of particles. Lu, et al. [46] proposed an equivalent simulation method to analyze particle behavior. In this method, the collision between particles is neglected. Based on the theory proposed by Lu, et al. some of the researchers further extended the simulation techniques. Based on the DEM simulation technique, Sanchez, et al. [47] simulated the dynamic characteristics of particle damper and impact damper. They noted that the dynamic characteristics of particle damper and particle impact damper are the same.

In recent years, graphics processing units (GPU) have significantly improved in simulating long data. GPUs can compute and process data quickly than CPUs [48]. Availability of modern computers and combination of CPU and compute unified device architecture (CUDA) made DEM simulations faster than before. In several simulations,

speed up of ten to hundred-folds has been achieved [49]. In our research, we performed an effective DEM implementation on CUDA-compatible GPUs to simulate the particle behaviors inside the rotary particle damper.

1.5 Experimental study in the field of prticle damping

Different researcher used different techniques to carry out extensive experiments on the performance analysis of particle dampers. Energy dissipation analysis of particles was conducted by Du, et al. [50]. Daniel [51] investigated the particle dampers based on analysis of shear strain gradient across the length of the cylinder. Zhang et al. [52] and Li, et al. [53] studied the effect of the mass ratio of particles on the performance of particle dampers. They suggested that particles with higher mass can provide more damping. Hollkamp, et al. [54] studied various design parameters, i.e., particle types, packing fraction, and random placement of particles at different locations of the damper, etc. Sathishkumar, et al. [55] investigated the effect of size of particles, the density of particles, and the hardness of particles.

There are two main factors to investigate the effect of particle damping. One is an external factor and other is an internal factor [56-58]. The external factors consist of excitation amplitude and frequency analysis. The internal factor consists of the type of particles, size of particles, size of cylinder, packing fraction, rotor speed, the shape of particles, and random placement of particles [59-61].

1.6 Applications of particle dampers

Particle damping technology has been studied for years, and it went through several developments and evolution phases. There are several engineering fields where particle dampers can be used, such as mechanical engineering, aerospace engineering, and civil engineering. Lu, et al. [62] proposed the idea of using particle dampers to control the unwanted vibration in the field of automobiles, rotating machines, airplanes, spacecraft, robotics, etc. Song, et al. [63] put forward the idea of using particle dampers in the mining truck vibration control. Haseena, et al. [64] used the particle damper for the vibration control of structures. They concluded that small size particles are capable of producing more damping than large size particles. Yang, et al. [65] used particle dampers in the vibration control of milling machine. Du, et al. [66] and Marhadi, et al.

[67] studied the use of particle dampers in cantilever beam vibration reduction. Effect of mass ratio, particle size, packing ratio, and frequency were analyzed. Xu, et al. [68] utilized the particle damper to reduce the noise and vibration of the banknote machine. Particle damping technology has been studied in the field of automobile engineering by Xia, et al. [69]. They used the particle damper to control the vibration of the drum brake. Zhang, et al. [70] proposed a particle damper to control the vibration of wind turbines. Jin, et al. [71] introduced the particle damper to reduce the vibrations of railway transient. Papalou, et al. [72] suggested the idea of using particle dampers to protect the historical buildings and statues from earthquake vibrations.

1.7 Objectives and scope of research

The main research objective of this study is to determine experimentally and numerically the performance parameters of the rotary elastomer particle dampers. The scope of the research is to perform the experimental and numerical investigation of the damper torque properties of rotary elastomer particle damper. An experimental setup is used to perform the experiments. The particle damper consisted of a rotating rotor. The particle damper was filled with silicon rubber elastomer particles. The objective was to investigate the effect of particle size, packing fraction, rotor speed, the shape of particles, and type of particles on the performance of the rotary elastomer particle damper on the torque. The visualization test and DEM analysis were conducted to understand the behavior of particles inside the rotary damper. The aim of this research is to gain a better understanding of the working mechanism and important factors which affect the damping performance of rotary elastomer particle dampers.

1.8 Organization of thesis

This dissertation consists of 5 chapters. Chapter 1 is about introduction, history, types and development of particle damper is discussed. Chapter 2 is about the torque properties of double-chamber rotary elastomer damper. It is found that, increase in packing fration, rotor speed, and size of elastomer particles increases the damper torque. The torque properties of single-chamber rotary elastomer damper are presented in Chapter 3. Shape of elastomer particles are inverstigated, increase aspect ratio of

elliptical particles decreases the damper torque. Spherical particles with aspect ratio 1:1 produced higher damper torque. Mix mode produce higher damper torque than spherical elastomer particles when the packing fraction is 60%. Chapter 4 details the investigation of using rotary damper with gap and no-gap between rotor anc cylinders. Size of elastomer particles plays significant role in producing higher damper torque in case of the damper with gap between rotor and cylinder. The damper with gap between rotor and cylinder produced higher damper torque when elastomer particles with 5 mm diameter are used. Finally, chapter 5 summarizes the work done and provides the final conclusion.

2. Experimental and Numerical Analysis of Double-Chamber Rotary Particle Damper

2.1 Introduction

In recent decades, the researchers have diverted their focus on particle dampers [6]. Particle dampers dissipate the kinetic energy of the system in two ways, one is due to collision between particle-particle and particle-wall of the damper, and the other is due to friction between particle-particle and particle-wall of the damper [69]. The main advantage of using particle dampers instead of oil damper is no leakage of oil. Even though different kind of expensive seals are used in oil dampers to prevent oil leakage, leakage occur in oil damper. Metallic particles have several disadvantages and one of them is noise due to collision between particles. Elastomer particles, due to high elastic behavior and low noise, can be useful in mechanical engineering applications.

In this section, experimental and numerical simulation approaches are used to analyze the damper torque characteristics of a novel double-chamber rotary elastomer particle damper. A rotary particle damper consists of a rotating shaft, which is connected to a rotor. Rotor moves with the rotation of shaft and pushes the elastomer particles to move forward in the direction of the rotor. Particles produce resistive forces in the motion of the rotor. Because of these resistive forced from particles, energy dissipation occurs, which results in the generation of damper torque. We investigated the effect of packing fraction, size of elastomer particles and rotational speed on damper torque of the novel double-chamber rotary elastomer particle damper. Quantitative and qualitative investigations of the rotary elastomer particle damper are conducted using the discrete element method (DEM). The main reason behind selecting this type of novel rotary elastomer particle damper is its simple working mechanism; small damper size allows it to be tested in real life applications, i.e., car seat suspension and door closer.

2.2 Experimental procedure

2.2.1 Fabrication of elastomer particles

Silicone rubber TSE3466 (Momentive) is used to fabirctae the particles. TSE3466 consists of TSE3466 A and TSE3466 B, which work as catalysts and are used to speed up the drying process. After mixing TSE3466 A and TSE3466 B, the liquid paste is inserted into the molds. We prepared elastomer particles of 3, 4, 5, and 6 mm diameter for our experiments to investigate the effect of size of elastomer particles on damper torque of rotary elastomer particle damper. The main reason to select particles of 3 mm diameter as the standard size is that we can expect higher damper torque of the damper due to higher deformation range compared to particles of 2 mm and 1 mm diameter. The second reason is that they are easy to fabricate. Figure 2.1 shows the outlook of elastomer particles used in our experiments.

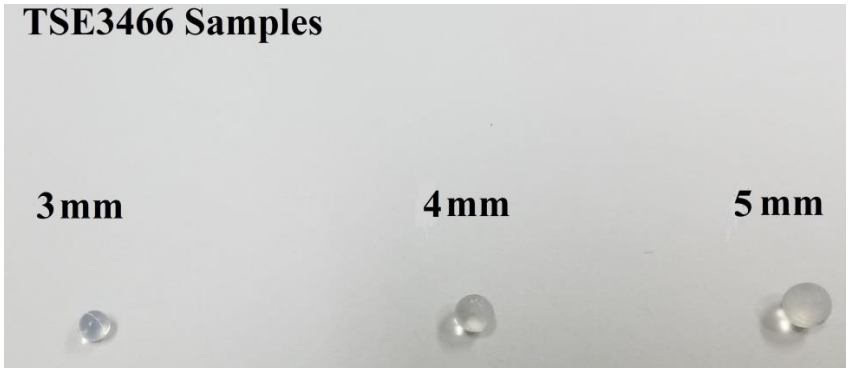

Fig.2.1 Elastomer samples of TSE3466 3 mm, 4 mm and 5 mm diameter particles after being removed from molds.

2.2.2 Double-Chamber rotary elastomer particle damper

Figure 2.2 shows the schematic diagram of the separated double-chamber rotary elastomer particle damper. There is a rotor connected to the main shaft. The damper is divided into two separated chambers, and particles in one chamber cannot move to another chamber, that's why the damper is named as double-chamber rotary elastomer particle damper. The bearings on both sides are used to support the shaft of the damper; two different bearings were used in this damper. To find the torque due to the friction between damper parts, the torque of the damper without inserting elastomer particles

was investigated and found that the torque is small enough to neglect. The rotary elastomer particle damper consists of a cylinder with covers, shaft, rotor which is fixed to the shaft, and the holder.

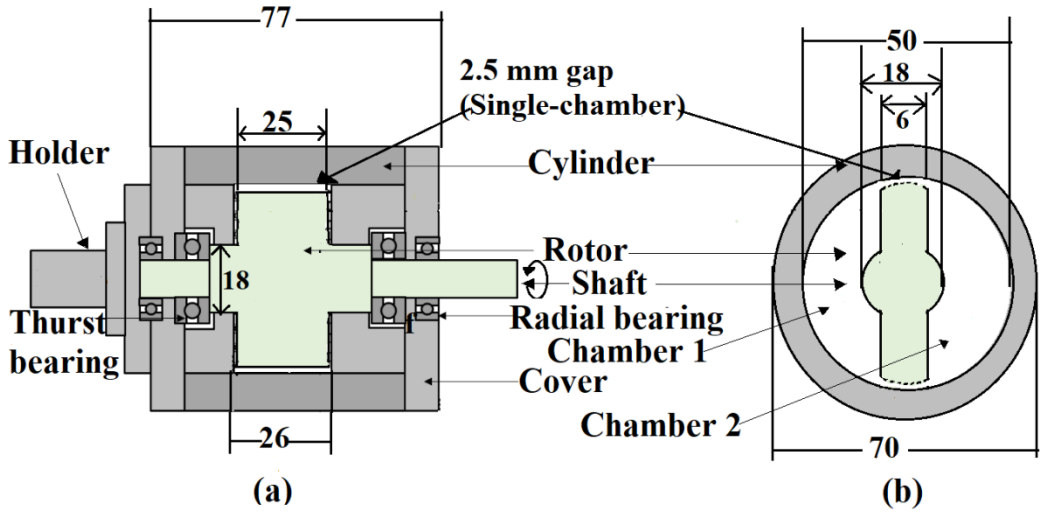

Fig. 2.2 Schematic diagram of the double-chamber rotary damper. (a) Cross-sectional side view and (b) cross-sectional top view.

2.2.3 Working mechanism of double-chamber rotary damper

The double-champer rotary elastomer particle damper is produced, experimentally torque characteristics of the rotary particle dampers are investigated. The particles from one chamber of the damper can not cross to the second chamber in double-chamber rotary elastomer particle damper, because the gap between the rotor and cylinder is small enough which particles can not pass through. Due to the resistive forces from particles, energy dissipation occurs, which results in the generation of damper torque [73, 74]. In double-chamber, because of two sections, particles are pushed from both sides. The elastic repulsion of particles is stronger in the double-chamber rotary elastomer particle damper than the single-chamber rotary elastomer particle damper. Hence, it is expected that double-chamber rotary elastomer particle damper can produce more damper torque than single-chamber rotary elastomer particle damper.

In this study, the effect of packing fraction and rotor speed on the damper torque is also analyzed. The packing fraction can be defined as $\emptyset=100M/V\rho$ [%], where $\emptyset$ is the packing fraction, M is the mass of the particle, V is the volume of the container (damper

body), and ρ is the density of particles.

2.2.4 Experiemental setup

Figure 2.3 shows the schematic diagram of the experimental setup on which the rotary elastomer particle damper was tested. A torque meter (UTM II, Unipulse Corporation) was used to measure the damper torque produced by the rotary elastomer particle damper. The rotational motion was provided to the damper with the motor. The shaft and the damper were connected with the couplings. The control unit controlled the rotational speed of the motor. The results were obtained by performing experiments three times on each prepared sample. Before starting experiments, 5 to 6 revolutions at high rpm were given to settle down the particles at random locations. The experiments were performed at each packing fraction till 20 revolutions of the shaft. The study on the effect of temperature on Young's modulus of Silicon was conducted by Ono [75]. He observed that minor decrease in Young's modulus was observed after 700-degree temperature rise. In the current research, the increase of temperature was checked during experiments by touching the damper; the increase in temperature was approximately few degrees. So the slight increase in temperature during experiments does not affect the mechanical properties of the TSE3466.

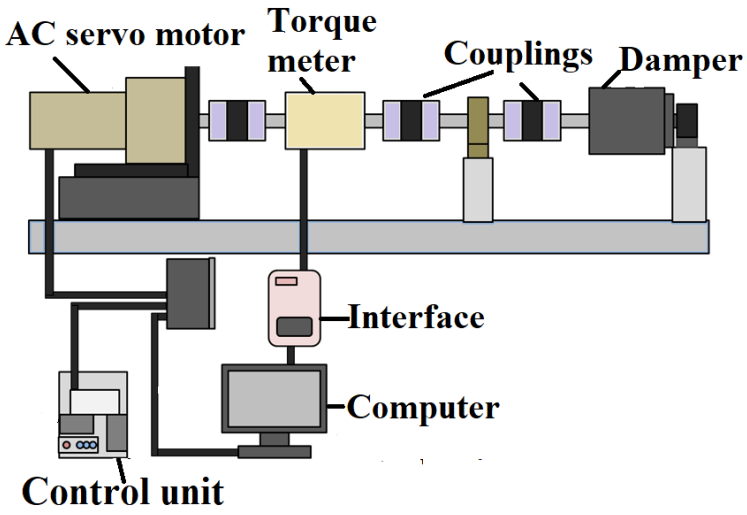

Fig. 2.3 Schematic diagram of experimental setup

2.3 Numerical simulation

To investigate the behavior of particles in the rotary elastomer particle damper, the DEM simulations were performed. The use of DEM to analyze behavior of particles has been increasing by the research community [76]. Much of the credited analysis of DEM technique to simulate the behavior of particles was conducted by Cundall and Strack [77]. Their contact force concept is shown in the Fig. 2.4 This model based on the Kelvin–Voigt material model, which consist of an elastic spring and a dashpot. This method is considered as the most successful model in the particle simulation analysis [78]. The particle behavior is analyzed based on Newton's second law of motion. The contact forces are calculated using the Voigt model, known as the spring dashpot system [79]. The DEM is widely used for the optimization of particle behavior, and the main advantage of this methodology is to obtain a qualitative and quantitative analysis of the system [80]. The model elaborates the normal and tangential forces acting on two spherical bodies in contact with each other. According to this model, normal contact force acts in the line of centers of the colliding particles, whereas the tangential contact force acts perpendicularly to the line of centers.

The basic equations of motions, can be stated that

$$m_i \frac{d^2 \boldsymbol{r}_i}{dt^2} = \boldsymbol{F}_i , \tag{1}$$

$$I_i \frac{d\boldsymbol{\Omega}_i}{dt} = \boldsymbol{T}_i , \tag{2}$$

where t is the time, m_i is the mass of the particle, $\boldsymbol{r}_i$ is the position vector of the particle i, $\boldsymbol{F}_i$ is the sum of the forces acting on the particle i, I_i is the moment of inertia, $\boldsymbol{\Omega}_i$ is the angular velocity vector, and $\boldsymbol{T}_i$ represents the total torque acting on the particles. In these equations, a particle is named as particle i, by considering which the model will further progress. $\boldsymbol{F}_i, I_i, \boldsymbol{T}_i$ can be expressed as

$$\boldsymbol{F}_i = \boldsymbol{F}_{cn} + \boldsymbol{F}_{ct} + \boldsymbol{F}_g, \tag{3}$$

$$\boldsymbol{T}_i = \boldsymbol{r}_i \times \boldsymbol{F}_{ct}, \tag{4}$$

$$I_i = \frac{8}{15}\rho\pi a^5, \tag{5}$$

$$\boldsymbol{F}_g = m_i \boldsymbol{g}, \tag{6}$$

where $\boldsymbol{F}_{cn}$ is the normal contact force between particles or the walls of the damper, $\boldsymbol{F}_{ct}$ is the contact force in tangential direction, $\boldsymbol{F}_g$ is the gravity force, $\boldsymbol{g}$ is the gravitational acceleration vector, a is the radius of the elastomer particle and ρ is the particle density. The contact force acting on the particles can be obtained from the model by Cundall and Strack [77]. This model is based on the Kelvin–Voigt material model [78], which consists of an elastic spring dashpot and a slider.

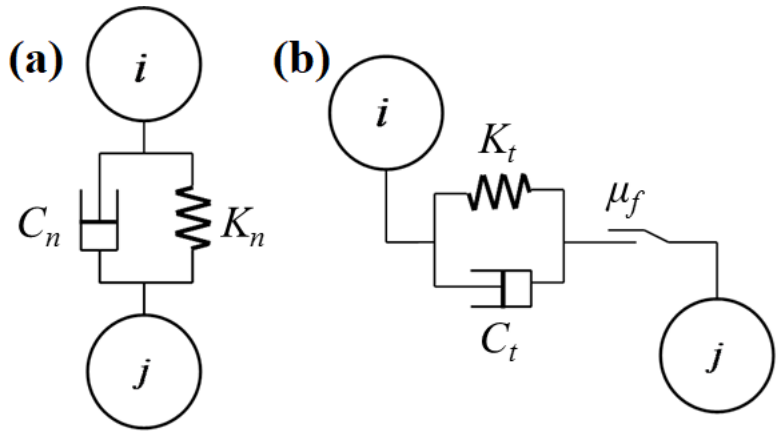

Fig.2.4 Contact force model of particle. (a) Normal direction, (b) Tangential direction

The contact forces $\boldsymbol{F}_{cn}$ and $\boldsymbol{F}_{ct}$ are given by

$$\boldsymbol{F}_{cn} = \left(-K_n\delta_n - C_n\boldsymbol{V}_{ij} \,.\, \boldsymbol{n}_i\right)\boldsymbol{n}_i, \tag{7}$$

$$\boldsymbol{F}_{ct} = -K_t\boldsymbol{\delta}_t - C_t\boldsymbol{V}_{fij}, \tag{8}$$

where the subscript n represents the parameters of normal direction, whereas the subscript t represents the parameters of tangential direction, K_n is the elastic modulus in normal direction, K_t is the elastic modulus in the tangential direction, C_n is the viscosity coefficient in normal direction, C_t is the viscosity coefficient in tangential

direction, δ_n is the strain in the normal direction, δ_t is the strain in tangential direction, $\boldsymbol{n}_i$ is unit vector in the normal direction from *i* to particle *j*, $\boldsymbol{V}_{ij}$is the relative velocity vector of particle *i* with respect to particle *j*, and $\boldsymbol{V}_{fij}$ is the tangential relative velocity.

$$\boldsymbol{V}_{ij} = \boldsymbol{v}_i - \boldsymbol{v}_j, \tag{9}$$

$$\boldsymbol{V}_{fij} = \boldsymbol{V}_{ij} - \left(\boldsymbol{V}_{ij}.\boldsymbol{n}_i\right)\boldsymbol{n}_i + 2a\left(\boldsymbol{\omega}_i - \boldsymbol{\omega}_j\right) \times \boldsymbol{n}_i, \tag{10}$$

where $\boldsymbol{\omega}_i$ and $\boldsymbol{\omega}_j$ are the angular velocity vectors of particles *i* and *j*, respectively. Viscosity coefficients in normal direction C_n and viscosity coefficient in tangential direction C_t can be represented as

$$C_n = \acute{\alpha}\sqrt{m_i K_n \delta_n^{0.25}}\,, \tag{11}$$

$$C_t = \acute{\alpha}\sqrt{m_i K_n \delta_{ct}^{0.25}}, \tag{12}$$

where δ_{ct} is the displacement in elastomer particle in tangential direction. $\acute{\alpha}$ determines the magnitude of viscous damper force, which can be expressed by following equation [29].

$$\acute{\alpha} = 2.2\sqrt{\frac{\ln(e^2)}{\ln(e^2)+\pi^2}}\,. \tag{13}$$

The elastic moduli in the normal direction are expressed by the following equations based on Hertz's contact theory,

$$K_{nij} = \frac{2}{3\pi}\left(\frac{1}{\delta_i}\right)\sqrt{\frac{a\delta_n}{2}}, \tag{14}$$

$$K_{niw} = \frac{4}{3\pi}\left(\frac{1}{\delta_i+\delta_w}\right)\sqrt{a\delta_n}\,, \tag{15}$$

$$\delta_i = \frac{1-\nu_i^2}{E_i\pi}, \tag{16}$$

$$\delta_w = \frac{1-\nu_w^2}{E_w\pi}, \tag{17}$$

where the subscript *w* indicates that the quantities relate to the wall, K_{nij} is the elastic coefficient when particle *i* and particle *j* are in contact whereas K_{niw} is the elastic coefficient when the particle *i* is in contact with the wall of the damper, E_i and E_w are the moduli of longitudinal elasticity of the particle and wall, respectively, and ν_i and ν_w are the Poisson's ratios of the particle and wall, respectively. Considering that there is no slip at the point of contact, the tangential elastic coefficients can be expressed as the following equations based on the Mindlin theory [80].

$$K_{tij} = \left(\frac{2\sqrt{2a}G_i}{2-\nu_i}\right)\delta_n^{0.5}, \tag{18}$$

$$K_{tiw} = \left(\frac{8\sqrt{a}G_i}{2-\nu_i}\right)\delta_n^{0.5}, \tag{19}$$

where K_{tij} is the elastic coefficient when particle *i* is in contact with another particle *j*. K_{tiw} is the elastic coefficient when particle *i* is in contact with wall of the damper. And G_i is the transverse elastic modulus of the particle, and is expressed as follows:

$$G_i = \frac{E_i}{2(1+\nu_i)}. \tag{20}$$

In this simulation, the elastic force and viscous force are taken into consideration in case of the normal direction as well as the tangential direction. For calculating the time steps of the velocity, displacement, and angular velocity of the particles, the Adams-Bashforth method of second-order accuracy was applied. The analytical model for the rotary elastomer particle damper is the same as the rotary damper prepared for experiments as shown in Fig. 2.5. The physical properties for the simulation were also the same as experiments. Table 2.1 shows the numerical conditions used for the simulation. Table 2.2 shows the mechanical properties used in the simulation. The friction coefficient was

taken 0.5 in this simulation [81]. The simulations were conducted at packing fraction of 30%, 40%, 45% and 50% with rotation speed of 60 rpm.

Table 2.1 Numerical conditions

Material	TSE3466 (Silicone rubber)
Packing fraction [Ø]	30%, 40%, 45% and 50%
Diameter of particles	3 mm, 4 mm, and 5 mm
Rotational speed	60 rpm
Time step	7.5×10^{-9} sec

Table 2.2 Mechanical properties of calculation

Density of particle [kg/m^3]	1.10×10^3
Particle's Poisson ratio	0.5
Wall's Poisson ratio	0.3
Friction coefficient (Particle-Particle)	0.5
Friction coefficient (Particle-Wall)	0.5

2.4 Results and discussion

2.4.1 Damper torque generation mechanism of double-chmaber rotary particle damper

The simulation results are shown in Figs. 2.5 and 2.6. To understand the compression force distribution on the particles, the simulations were conducted at Ø=45% and Ø=30% with the rotational speed of 60 rpm. From Figs. 2.5 and 2.6, high compressive force on the particles depends on the angle of the rotor. When the rotor moves, it pushes the elastomer particles in contact with the rotor. Particles in contact with the rotor push other particles. The compressive forces on the particles are investigated using simulation results. From Figs. 2.5 and 2.6, there are many particles with strong compressive forces near the rotor, due to which repulsive force from the particles to the rotor becomes strong. When the rotor is at the bottom region, the compressive force of particles is strong because the gravitational force is also acting on the particles. When the rotor is in the vertical position, as shown in Figs. 2.5(a) and 2.6(a), the gravitational force pushes the particles downward (away from the rotor), so

there are weak compressive forces of the particles. The drop of particles from the top of the cylinder to the bottom of the cylinder provides the time delay of particle deformation to the motion of the rotor.

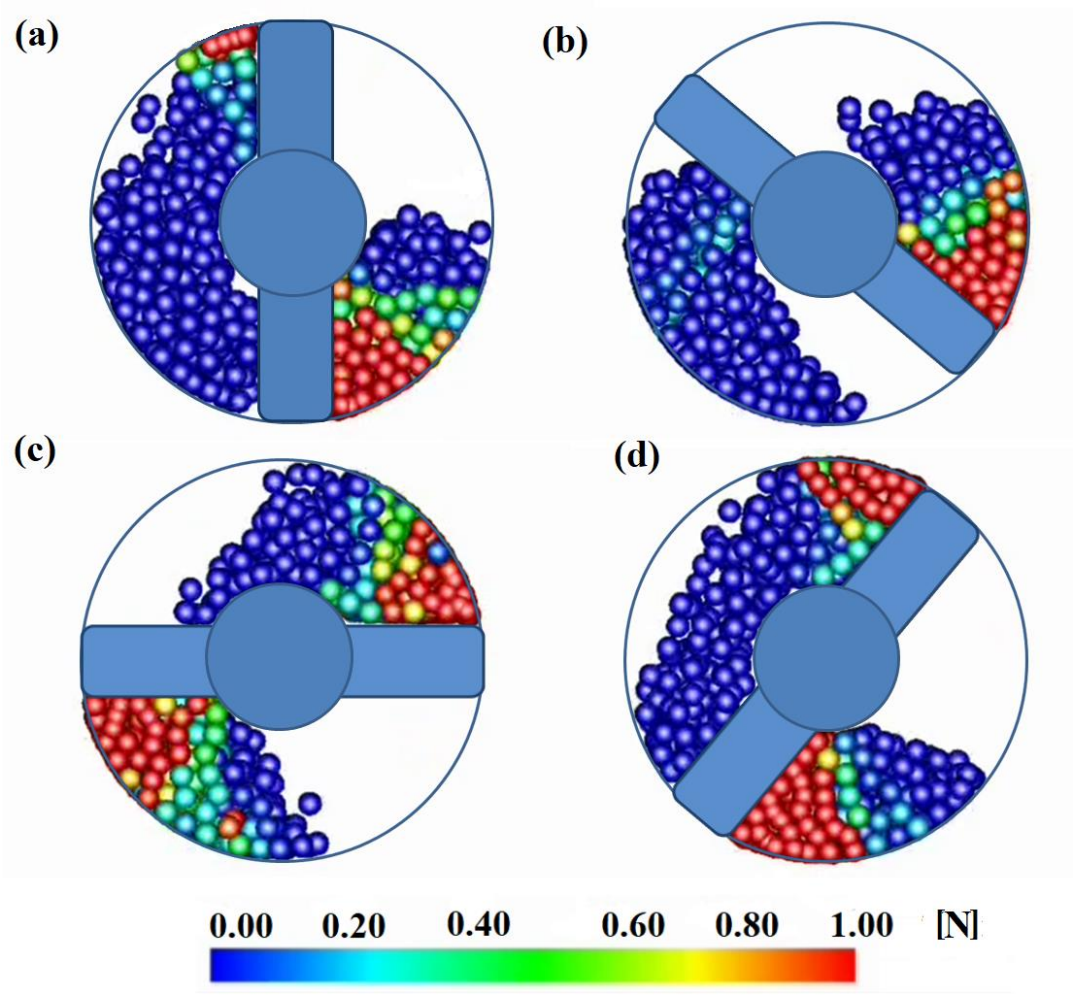

Fig. 2.5 Compressive force acting on the particle, ∅=45 % and the rotational speed of 60 rpm (a) 0 degree, (b) 45 degree, (c) 90 degree, (d) 135 degree. The direction of rotation is counter-clockwise.

From Figs. 2.5 and 2.6, when the rotor angle is the same in both cases, the compressive force of particles with 45% packing fraction, is higher than that with 30% packing fraction. An increase in packing fraction increases the number of particles which increases the elastic repulsive force. When the packing fraction is higher, the number of particles increases, and the empty space inside the damper becomes small. When the packing fraction is low, the particles move toward the empty space inside the damper. In other words, the damper torque increases when large numbers of particles

are used because the increase in the number of particles increases the particle-particle and particle-wall contacts, which produces larger frictional forces.

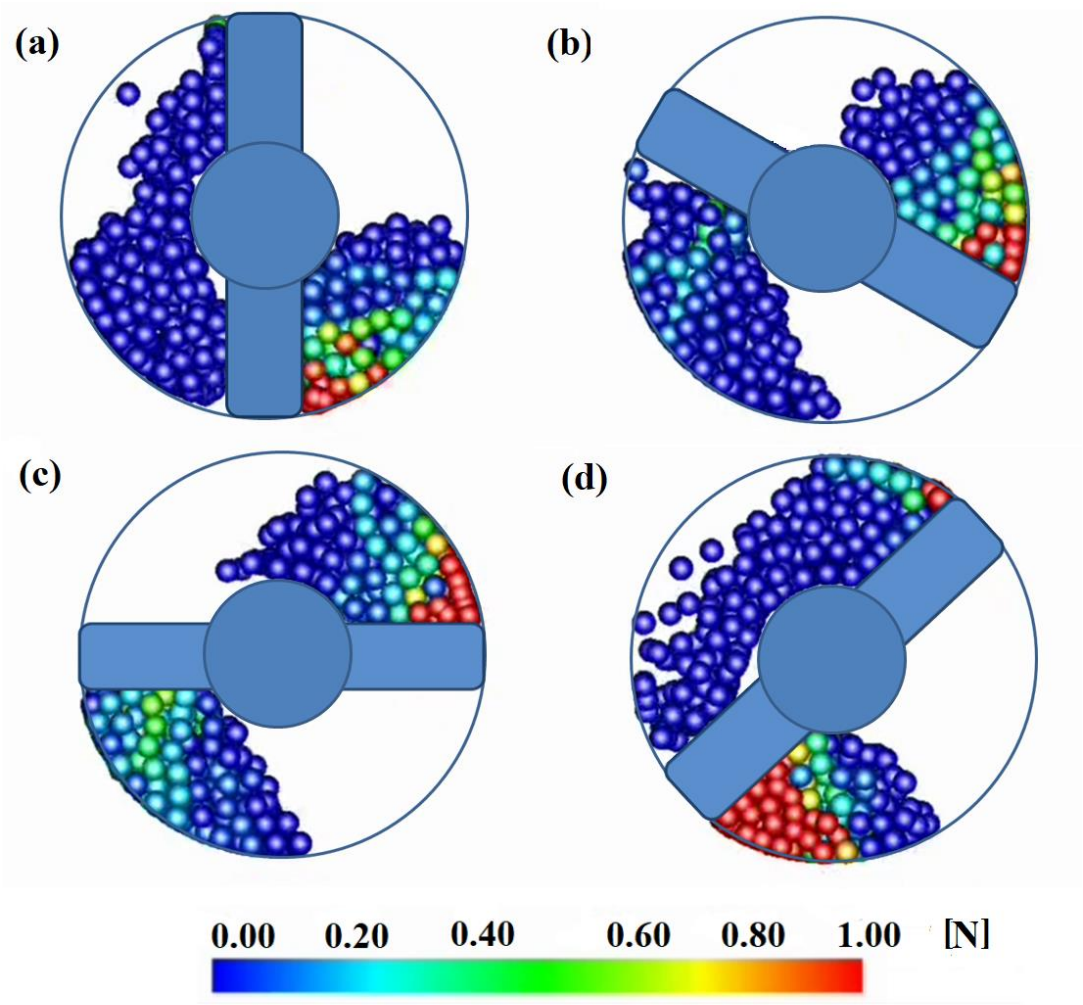

Fig. 2.6 Compressive force acting on the particle, ∅=30 % and the rotational speed of 60 rpm (a) 0 degree, (b) 45 degree, (c) 90 degree, (d) 135 degree. The direction of rotation is counter-clockwise.

Figure 2.7 shows the torque vs. packing fraction as the typical case at the rotational speed of 60 rpm by varying the packing fraction and comparing the experimental results with simulation results. The tendency of the simulation results is the same as the experimental results. The Experimental results are slightly larger than the simulation results. The simulation results are qualitatively in good agreement with experimental results. One of the possible reasons behind the slight difference in

simulation and experimental results is the surface roughness of the particles and wall. The surface roughness factor is not considered in this simulation

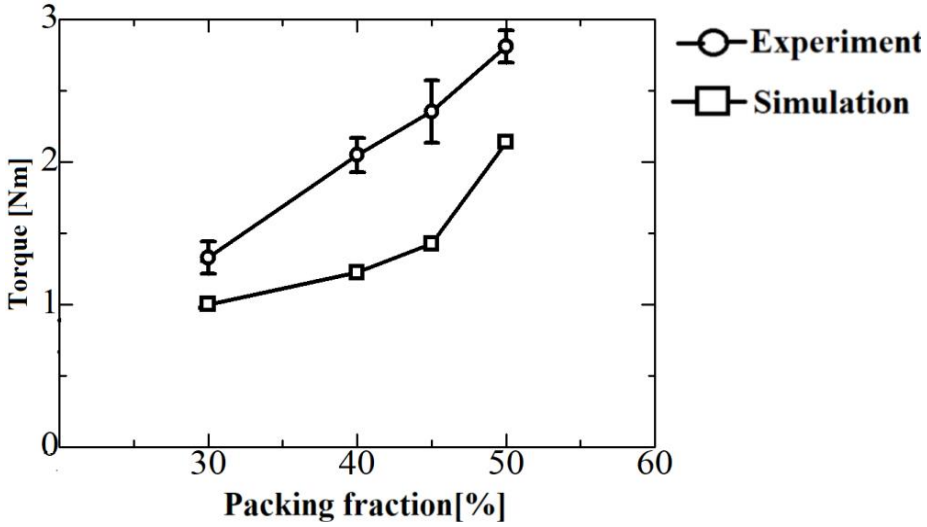

Fig.2.7 Experimental and simulation results of the torque versus packing fraction curve using elastomer particles of 3 mm diameter. The rotational speed is 60 rpm.

2.4.2 Effect of paking fraction and rotor speed on damper torque

Figure 2.8 shows the torque vs. packing fraction graph of the double-chamber rotary elastomer particle damper. Spherical elastomer particles of 3 mm diameter particles were used in this invesigtaion, because sperical elastomer particles are capable of producing higher damping in particle damper compare to other shapes [82]. There is the increase in damper torque as the packing fraction increases. The main reason for the decline in damper torque with the decrease of packing fraction is caused by the decrease in the number of particles. When the number of particles decreases inside the damper, the number of collisions between particles also decreases [83]. Friction also plays a significant role at high packing fraction; when particles are in close contact with each other, strong normal and tangential forces act on the particles [84]. Less friction between particles affects the damper torque because particle behavior is influenced by the normal interaction forces [85].

When the packing fraction decreases, the total volume of void space in the damper increases. When the rotor pushes elastomer particles, the particles move to fill the gap of the damper. However, the empty space remains in the backside of the rotor. To understand this phenomenon, we compare the cases of 30% and 50% packing fractions.

In the case of 30% packing fraction, empty space exists inside the damper, while this space is very less in the case of 50% packing friction, as shown in Fig 2.9. At 30% packing fraction, when forces are acting on the particles by the rotor, the particle utilizes the available space inside the damper and move toward empty space; that is, in the case of 30% packing fraction, weak compression force acts on the particles.

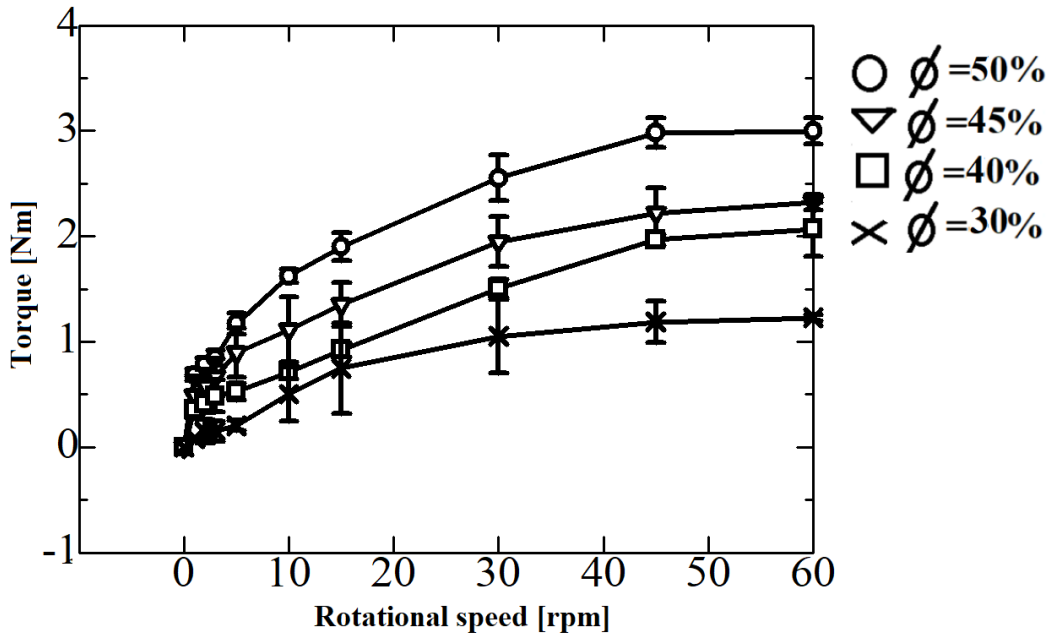

Fig. 2.8 The torque versus rotational speed curve when the diameter of particles is 3 mm

In the case of 50% packing fraction, the particles are strongly compressed because of the quite small empty space available inside the damper (Fig 2.9), so the damper force is strong due to the strong frictional and elastic forces. From Fig. 2.8, Ø = 50% higher damper torque of 2.998 Nm is obtained at the rotational speed of 60 rpm, and as the packing fraction decreases to 45%, 40%, and 30%, the maximum damper torque also decreases to 2.323 Nm, 2.167 Nm and 1.328 Nm even at the same rotational speed of 60 rpm.

Damper torque also depends on the rotational speed of the damper, as shown in Fig.2.8. With the increase of rotational speed of the rotor, an increase in the damper torque is observed. One of the main reasons is that the forces acting on the particles are weak at low rotational speed because when the rotor pushes the elastomer particles, they utilize the space inside the damper and move towards that space. At the high rotational

speed of the rotor, particles do not have time delay to move toward the available space inside the damper. The second reason is the more number of impacts between particles at the high rotational speed of the rotor. High speed rotor pushes the elastomer particles with higher velocity and particles impact with other particles and transfer of energy occur between particle-particle and particle-wall.

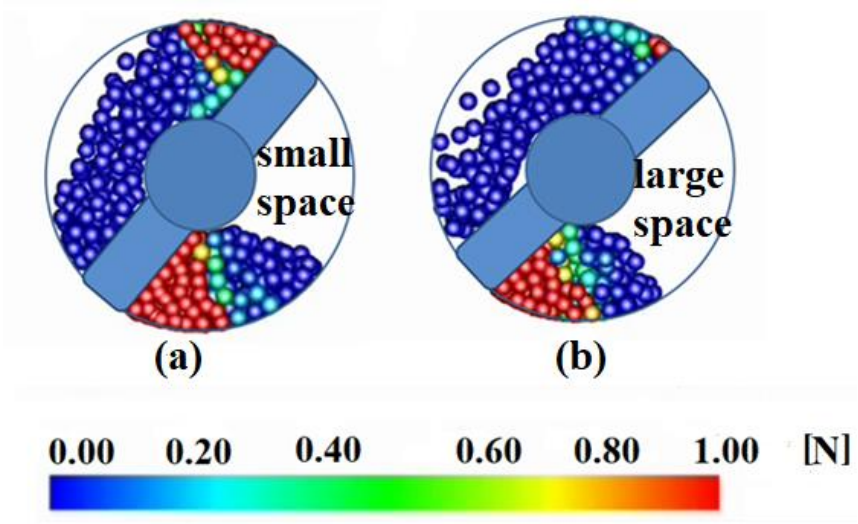

Fig.2.9 Simulation results at 50% and 30% packing fraction (a) more number of particles under compression 50% packing fraction, (b) less number of particles under compression at 30% packing fraction.

2.4.3 Effect of size of elatomer particles on damper torque

The double-chamber rotary damper using the particles with diameters of 3 mm, 4 mm, 5 mm, and 6 mm was experimentally tested. In this section, a correlation between the damper torque and the size of elastomer particles is demonstrated. The increase of damper torque was observed due to the increase in the size of the elastomer particles. Figure 2.10 shows the damper torque in cases of the particle with 3 mm, 4 mm, 5mm, and 6 mm diameter at 60 rpm. The size of elastomer particles plays a significant role in increasing the damper torque of the rotary elastomer particle damper. From Fig. 2.10, the decline in the damper torque is observed when small diameter particles are used. Damper torques produced by the damper using the particles with 6mm, 5 mm, 4 mm, and 3 mm diameter particles at the packing fraction of 50% are 6.163 Nm, 4.128 Nm, 3.216 Nm, and 2.998 Nm, respectively. The main reason behind the increase of the damper torque with the increase of particle size is the larger deformation capability in

large-sized particles. Larger particles produce stronger frictional forces acting on each other and on the damper wall surface. Larger particles have more contact areas, which results in the generation of high frictional forces. The diameter of elastomer particles and damper torque directly correlate with each other.

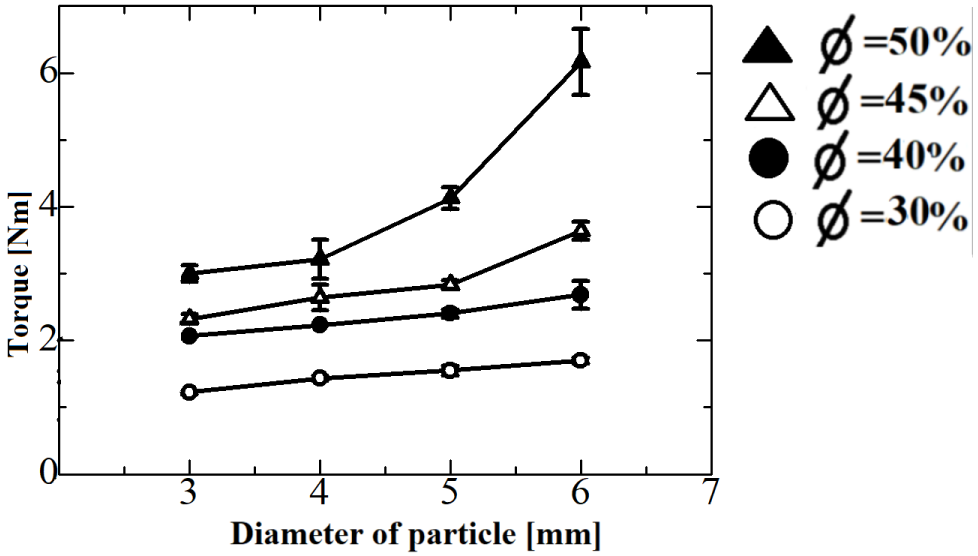

Fig.2.10 The torque versus diameter of the particle curve at 60 rpm, using particles with 3 mm, 4 mm, 5 mm and 6 mm diameter

2.5 Conclusion

In this section, the separated double-chamber rotary elastomer particle damper was prototyped and experimentally tested. The damper torque characteristics were examined by varying the packing fraction, size of particles and rotational speed of the rotor. The DEM analysis was performed for investigation of the particle behavior in the rotary elastomer particle damper. Particles infront of the rotor contributes more in generation of damper torque than the particles away from the rotor. Particles away from the rotor support the particles infront of the rotor. Gravity plays a significant role in incrasing and decreasing the damper torque according to location of the rotor inside the dampr. The simulation results agree well with the experiment results. It is clear that, increase in packing fraction, rotational speed of the rotor and size of the elastomer particles resulted in an increase in damper torque of rotary elastomer particle damper.

3. Experimental and Numerical Analysis of Single-Chamber Rotary Particle Damper

3.1 Introduction

In this section, the effect of using spherical and ellipsoidal elastomer particles (with different aspect ratios) on damper torque of rotary elastomer particle damper is investigated. The aspect ratio denotes the ratio of the major axis to the minor axis. The ellipse with an aspect ratio of 1:1 is a sphere. The effect of aspect ratio in a rotary elastomer particle damper has never been studies before; as well as the effect of mixing of spherical and ellipsoidal elastomer particles with 50:50 ratios can provide new insight to the research on particle dampers. It is hypothesized that the spherical elastomer particles in the rotary particle damper provide a strong damper torque than ellipsoidal elastomer particles. The mixture of spherical and ellipsoidal elastomer particles in the rotary particle damper may provide strong damper torque than the spherical elastomer particles. The main reason to select this type of rotary damper is its simple working mechanism. More number of particles can be accumulated in single-chamber rotary elastomer particle damper than the double-chamber rotary elastomer particle damper of same size. The single-chamber rotary damper can have several mechanical engineering applications, i.e., car seat suspension or automobile door closer because of its small size and simple structure. In the future, the prototype can easily be tested for practical application due to its small size. The effects of packing fraction; rotor speed and aspect ratio of particles on the damper torque of rotary elastomer particle damper are examined. To understand the behavior of particles inside the damper, the numerical simulations using the discrete element method and visualization experiments are performed.

3.2 Experimental procedure

3.2.1 Fabrication of elastomer particles

TSE3466 is also used to investigate the effect of different shapes of elastomer particles on damper torque of rotary elastomer particle damper. TSE3466 is used to prepare elastomer particles with aspect ratios 1, 1.2, and 1.5. The effect of mixing the spherical and ellipsoidal particles at 50:50 ratios is also investigated. Figure 3.1 shows

the outlook of the elastomer particles used in our experiments. Some particles were colored in black and red for use in visualization experiments.

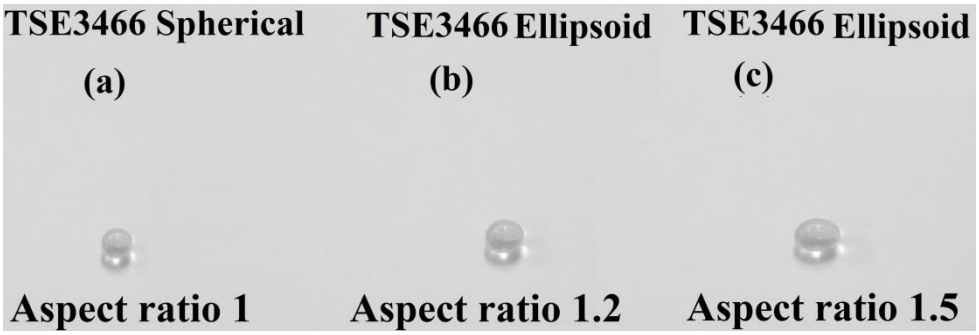

Fig.3.1 Elastomer samples of TSE3466 particles, (a) spherical particles, and ellipsoidal particles with aspect ratio (b) 1.2 and (c) 1.5.

TSE3453 and TSE3466 are used to investigate the effect of different types of materials on the damper torque of rotary elastomer particle dampers. TSE4553 is also a silicon rubber produced by Momentive Performance Material Company. The density of TSE3453 and TSE4366 is the same, while the tensile strength and hardness are different from each other. The basic properties of TSE3453 are shown in Table.3.1.

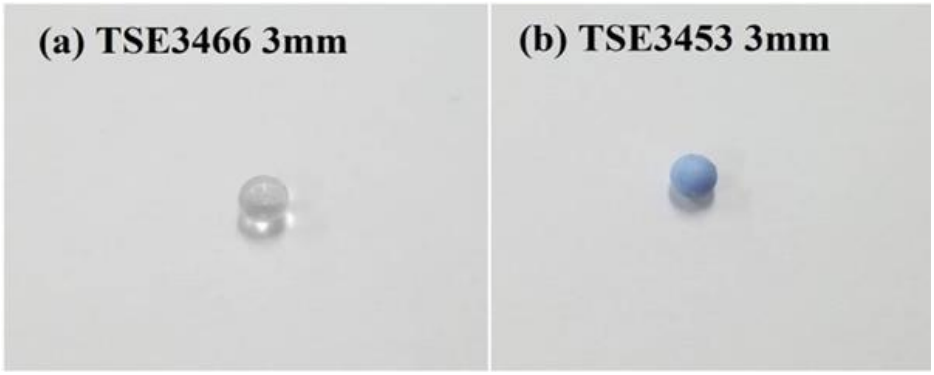

Fig.3.2 Outlook of the elastomer particle made of TSE3466 and TSE3453 with 3 mm diameter

Table.3.1 Properties of TSE3466 and TSE3453

Material	Density	Shore hardness (A)	Tensile strength [MPa]
TSE3466	1.10	60	7.4
TSE3453	1.10	40	6.4

3.2.2 Single-chamber rotary elastomer particle damper

Figure 3.3 depicts the schematic diagram of the single-chamber rotary elastomer particle damper. To examine the torque due to the friction between damper parts, the damper's torque without inserting particles was investigated and perceived that the torque is negligible. The rotor used in this design is rectangular, and it is placed 2 mm offset from the axis of the damper. The rotor is fixed onto the rotor shaft with the help of a groove. The shaft provides rotational motion to the rectangular rotor of the damper. The rotor is supported by bearings (NTN 30202) on both sides. This bearing has the ability to sustain both axial and radial loads, which makes it suitable to be used in this rotary elastomer particle damper. A holder is used on one of the covers to hold the damper from rotation during experiments. SAE304 grade stainless steel is used to make the parts of the damper.

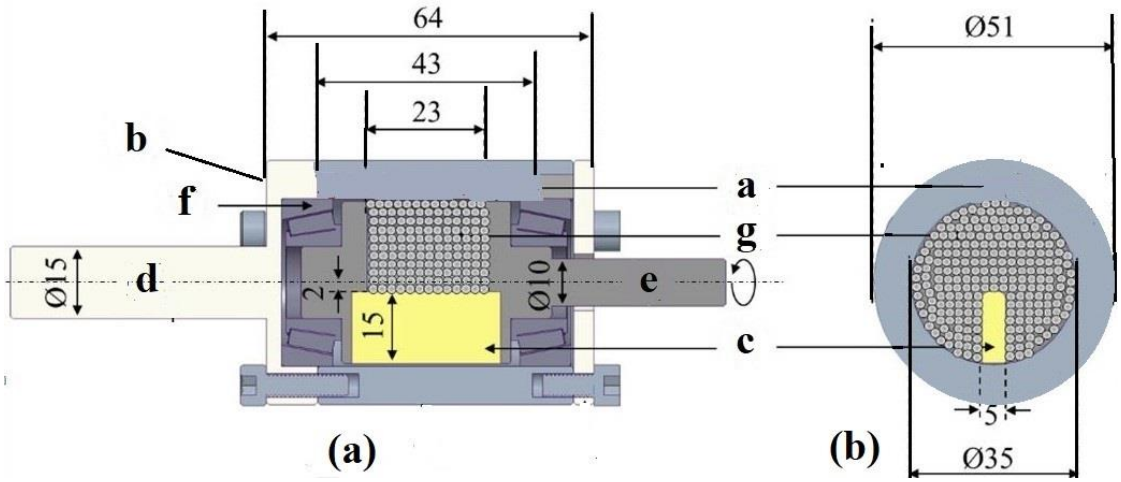

Fig.3.3 Schematic diagram of the single-chamber rotary particle damper: (a) cross-sectional side views of the damper. (b) cross-sectional top views of the damper. a. body, b. cover, c. rotor, d. holder, e. shaft, f. bearings, g. elastomer particles

3.2.3 Working mechanism of single-chamber rotary damper

The rotary damper was prepared to investigate damper torque properties due to different shapes and types of elastomer particles. The particles inside the damper generate resistive forces in the direction of the motion of the rotor. In order to continue its motion, the rotor needs to apply forces to overcome the resistive forces produced by the

particles. Due to the resistive forces from particles, energy dissipation occurs, which results in the generation of damper torque [73, 74]. In a single-chamber rotary elastomer particle damper, the repulsive forces from the particles can be produced due to elastic deformation and collision of particle-particle and particle-wall of the damper. When the rotor moved the particles deformed due to forces from neighboring particles, rotor, and walls of the damper.

3.2.4 Experiemental setup

Figure 3.4 is the schematic diagram of the experimenta1 setup used in this research. The torque meter (UTM II, Unipulse Corporation) was used to measure the damper torque. The motor was used to rotate the shaft of the damper. The shaft and damper were joined together with couplings. The control unit controlled the rotational speed of the motor. The results were obtained by performing experiments three times on each prepared sample. Before starting experiments, 5 to 6 revolutions at high rpm were given to settle down the particles at random locations. The experiments were performed at each packing fraction till 20 revolutions of the shaft. In this study, the increase in temperature of the cylinder of the damper was monitored during the experiments. Few degrees rise in temperature was detected, however, it did not change the mechanical properties of TSE3466, so the effect of temperature can be negligible.

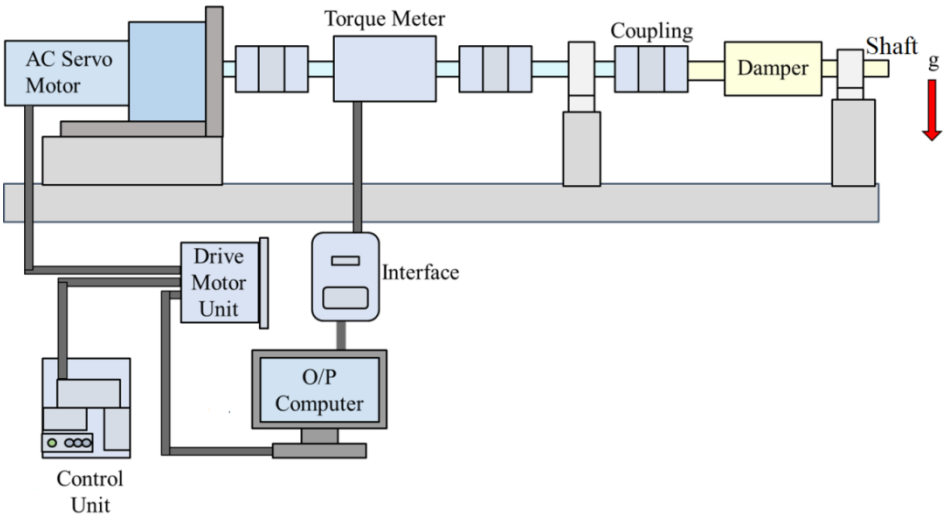

Fig. 3.4 Schematic diagram of experimental setup

3.3 Numerical simulation and visualization of the single-chamber rotary elastomer particle damper

3.3.1 Numerical simulation

The DEM by Cundall and Strack [77] is a well-known tool for simulating particle behavior. DEM community faced problems in simulating non-spherical particles. Thus, the DEM is used only for analysis of the behavior of spherical elastomer particles, whereas the visualization technique is used to understand the behavior of ellipsoidal elastomer particles. The DEM is based on Newton's laws of motion which is explained in detail in the previous section 2.3. According to the model, normal contact force acts in the line of centers of the colliding particles, whereas the tangential contact force acts perpendicularly to the line of centers. For calculating the velocity, displacement, and angular velocity of the particles, the Adams-Bashforth method of second-order accuracy was used. The simulation was conducted at the packing fractions of 40%, 50%, 55% and 60%. The particle diameter was 3 mm and the rotor speed was 60 rpm. The friction coefficient was 0.5 in this simulation [81], and the time step was 7.5×10^{-9} sec. The density of particle was 1.10×10^{3} kg/m^{3}. Particle's Poisson ratio and wall's Poisson ration were 0.5 and 0.3. The analytical model for the rotary elastomer particle damper was the same as the rotary damper used for experiments as shown in Fig. 3.3.

3.3.2 Visualization experiments

Visualization tests were conducted using transparent damper bodies and observations were made by naked-eye, and video recording. We conducted numerical simulations as well visualization in which the damper body was prepared of an acrylic transparent material. The visualization provided cognitive visual cues for the in-depth analysis of the motion of the particles. The video of the elastomer particle motion showed seemingly random motion, with some particles having small displacement compared to other particles. Video recording helped to extract and present serial images pairs of time separation from the videotaped sequence. It seemed difficult to keep track of the motion of particles because all particles look similar in color and shape, thus

some colored particles were prepared and mixed with other particles, which made visual study a lot easier. Particle's motion of the single-chamber rotary elastomer particle damper was observed at 60 % packing fraction at 1~60 rpm. Particles were observed till the 20 complete rotations of the rotor. It was impossible to observe the particles' motion at normal rotational speed, so slow-motion videos were recorded. By watching slow-motion videos, it was concluded that the basic behavior of particles inside the damper at high rotational speed remains the same as low rotational speed. High rotational speed only increases the speed of the motion.

3.4 Results and discussion

3.4.1 Visualization of behavior of spherical particles

Figure 3.5 shows the visualization of the behavior of the spherical particles at the rotor speed of 60 rpm and 60% packing fraction. Sequential photos were taken from the video at every 0.01 sec. We focused on the motion of the particle *i.* From Fig. 3.5 (a), where the rotor of the damper can be seen easily; this is the location where particle *i* appears on the screen at time *t*=0.01 sec. At time *t*=0.02 sec, particle *i* collides with a colored particle; we name it particle *j* as shown in Fig. 3.5 (b). After a collision at *t*=0.03 sec, particle *j* scatters away from particle *i* at a very high velocity, as shown in Fig. 3.5 (c). At *t*=0.06 sec particle *k* collides with particle *i* as shown in Fig. 3.5 (f). Due to this collision at *t*=0.07 and 0.08 sec, particle *k* bounces back towards the bottom of the cylinder, as shown in Fig. 3.5 (g) and (h). At time *t*=0.10 sec, the particle *i* is in contact with another colorless particle *l* as shown in Fig. 3.5 (j). Particle *i* and particle *l* collide with each other at *t*=0.11 and *t*=0.12 sec and both particles start to bounce back from each other due to collision, as shown in Figs. 3.5 (k) and (l). At time *t*=0.14 sec, particle *i* is collides with a new colored particle *m*; particle *i* and *m* does not bounce back from each other and keep on moving forward by applying strong compressive forces on each

other. Due to high-intensity forces, deformation in their shapes can be seen in Figs. 3.5 (n) and (o). At time *t*=0.15 sec, the particles are strongly compressed, however, they are rotating each other because of which frictional forces are produced.

It is observed from the visualization that the particles near the rotor are strongly compressed than the particles away from the rotor. The particles near the rotor apply repulsive forces by applying strong compressive forces. The particles away from the rotor apply repulsive forces due to collision between particles. Repulsive forces from the particles resist the motion of rotor and frictional forces are produced. Particles near the rotor have strong compressive forces because they are supported by the other particles. So the damper torque is produced due to repulsive forces from the particles. Repulsive forces are produced due to collision and compression between particles.

3.4.2 Visualization of behavior of ellipsoidal particles

From Fig. 3.6(a), the particle *i* can be seen on the screen, particle *i* keeps on moving forward with a rolling motion, as shown in Fig.3.6 (b). As the particle *i* moves forward, it comes in contact with the particle *j* and *k*, as shown in Fig. 3.6 (c). After collision with the particle *i*, the particle *k* bounces back, however, the particle *j* keeps in contact with the particle *i*, and they apply compressive forces on each other as shown in Fig. 3.6 (d). At time *t*=0.08 sec, the particle *i* comes in contact with particle *l* and *m*. The particles *l* and *m* are applying strong compressive forces on the particle *i*, because of deformation in the particles. They do not separate from each other because of lack of collision and rolling motion, as shown in Figs. 3.6 (h) and 3.6 (i). After contacting with the particle *i*, the particles *m* and *l* do not bounce back. After this point, no more collisions are observed because the particles are into a jammed state. The particle *i* moves forward while being in contact with the particles *l*, *m*, and *n* from Fig. 3.6 (j) to 3.6 (o). One important thing is noticed in Figs. 3.6 (m), (n) and (o) that dense cluster of particles is formed where they stop to rotate.

The ellipsoidal elastomer particles have less number of collisions than that of spherical particles and the rotational motion between ellipsoidal particles is less than that of the spherical particles. The numbers of collisions are less in the ellipsoidal particle due to less rotational motion between particles. The ellipsoidal particles have less rotation due to line contact with each other and walls of the damper. The line contact between particles produces an interlocking between particles which enable them to rotate each other. In other words, the contact surface between ellipsoidal particles is more than the spherical particles [82]. Increase in contact surface produces friction in rotation between ellipsoidal particles. In spherical particles contact surface is smaller than that of the ellipsoidal particles, which let them easy to rotate each other. In a particle damper for producing higher damper torque, it is important that particles have compressive forces while having rotational motion between each other. When particles are strongly compressed than the numbers of collisions between particles reduce. From Figs. 3.6 (m), (n) and (o), in case of ellipsoidal particles the strong compression region is formed. There are more number of collisions of spherical particle *i*, whereas number of collision of ellipsoidal particle *i* are significantly less than the spherical particle.

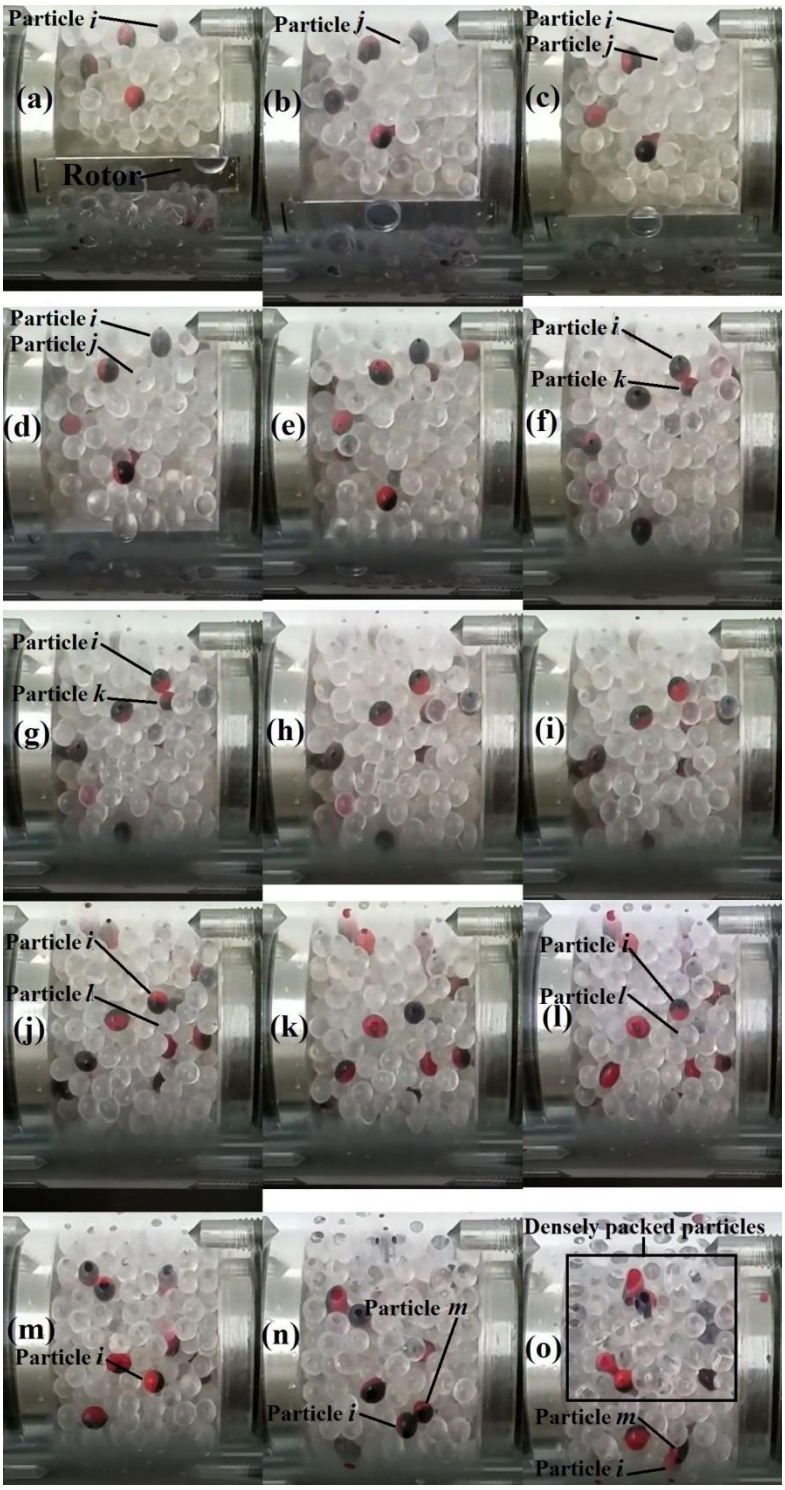

Fig. 3.5 Visualization of spherical particles at 60 % packing fraction, *t* = (a) 0.01, (b) 0.02, (c) 0.03, (d) 0.04, (e) 0.05, (f) 0.06, (g) 0.07, (h) 0.08, (i) 0.09, (j) 0.10, (k) 0.11, (l) 0.12, (m) 0.13, (n) 0.14, (o) 0.15 sec.

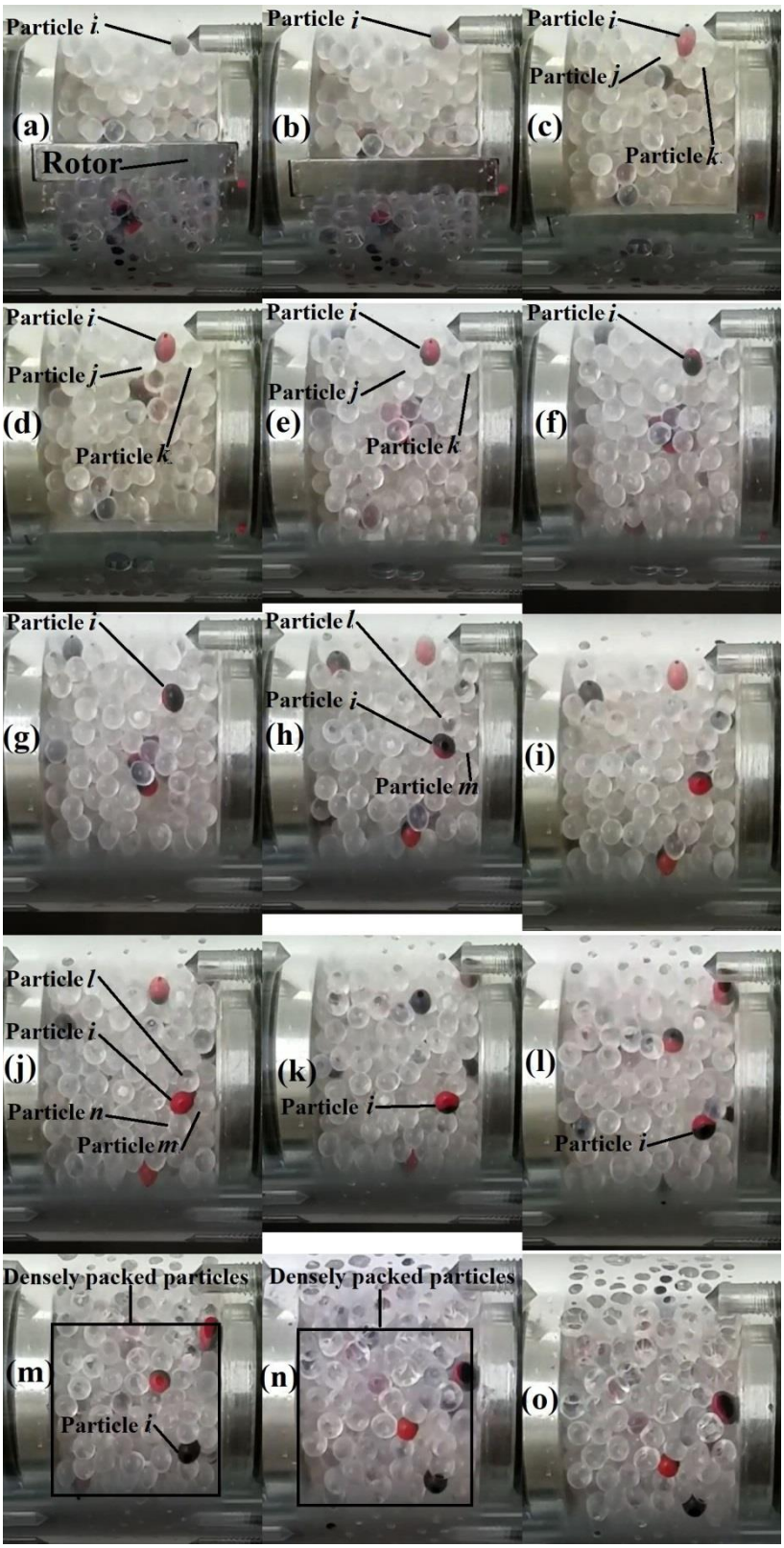

Fig. 3.6 Visualization of ellipsoidal shape particles at 60 % packing fraction, t = (a) 0.01, (b) 0.02, (c) 0.03, (d) 0.04, (e) 0.05, (f) 0.06, (g) 0.07, (h) 0.08, (i) 0.09, (j) 0.10, (k) 0.11, (l) 0.12, (m) 0.13, (n)

0.14, (o) 0.15 sec.

3.4.3 Damper torque generation mechanism of single-chamber rotary particle damper

The behavior of elastomer particles and the compressive force acting on the elastomer particles were analyzed based on the simulations as shown in Fig. 3.7. The damper produces a damper torque because of elastomeric forces generated due to compression of the particles and the frictional forces between particle-particle and particle-wall. Particles near the rotor have high compressive force because of the strong forces from the rotor. Particles near the rotor are also supported by other particles. Particles produce repulsive forces, which create resistance in the motion of the rotor. Repulsive forces applied by the particles are produced due to friction and collisions between particle-particle and particle-wall. Gravity also plays a significant role in increasing the damper torque. The compressive force between particles is actually pressing the particles against the wall, and the increase of frictional force occurs, so the repulsive force applied by the particles on the rotor, due to which damper torque produces. From Fig. 3.7, the distribution of strongly compressed particles changes according to the angle of the rotor. The particles in contact with the rotor have strong compressive force. At 90 degree and 180 degree angles of the rotor, the compressive force of the particles becomes strong due to gravitational force. The gravitational force resists the particle's motion, and particles apply strong repulsive forces on the rotor. When the rotor is at 270 degree, the particles drop from top to bottom on the left side due to gravitational force. Gravity pushes the particles away from the rotor, so the weak compression forces can be seen at 270 degrees. The compressive force is stronger at 0 degree than 270 degrees because at 0 degree; the gravity is acting on the particles in downward direction. Gravity holds the particles which incrases the frictional force.

Other particles support the particles around the rotor, so the strong compressive forces can be seen in Fig. 3.7 (a). Figure 3.8 shows the torque vs. time graph of simulation and experimental results of spherical particles at a rotor speed of 60 rpm. The fluctuation in the damper torque at different time steps is due to the different angles of the rotor. The strong damper torque seems to be at the 90 degree angle of the rotor because large numbers of particles are strongly compressed, as shown in Fig 3.7 (b). Damper torque is weak at the 270 degree angle of the rotor because the number of strongly compressed particles is less, as shown in Fig. 3.7 (d).

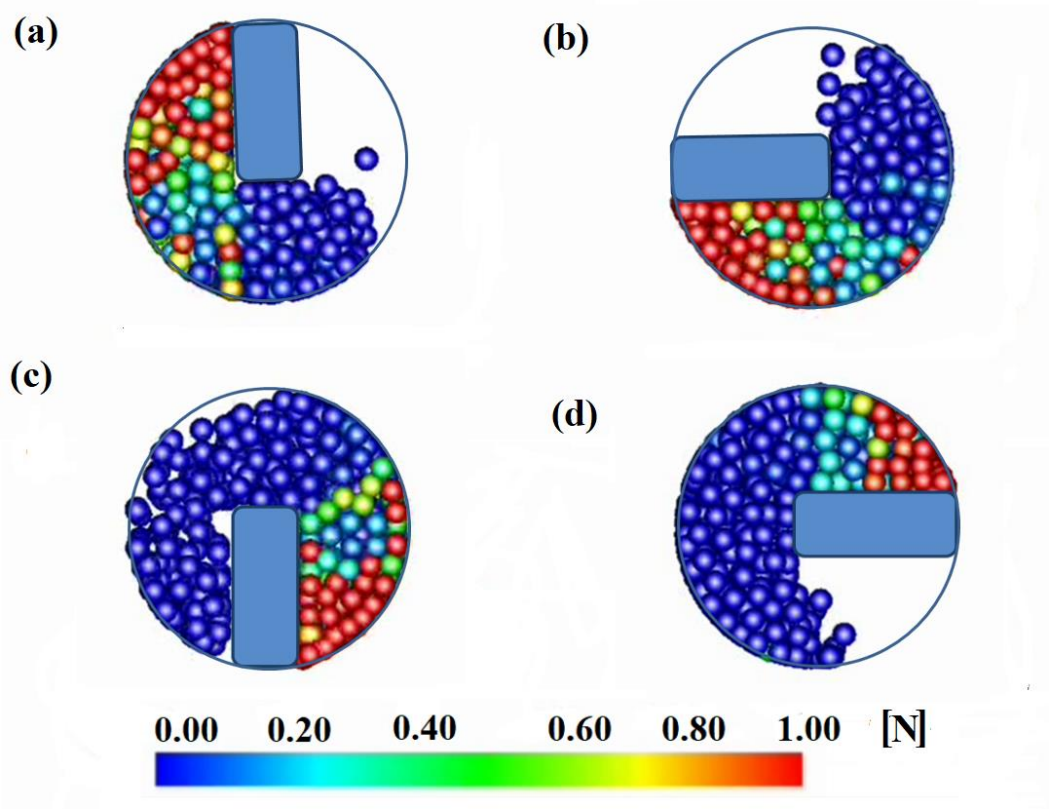

Fig.3.7 Compressive force acting on the particle, ∅=60% and the rotor speed of 60 rpm, the angles of the rotor are (a) 0 degree, (b) 90 degree, (c) 180 degree, and (d) 270 degree. The direction of rotation is counter-clockwise.

Figure 3.9 shows the torque vs. packing fraction graph for comparing the simulation and experimental results of spherical particles at rotor speed of 60 rpm. The tendency of the simulation curve is almost the same as the experimental curve. The simulation results show a slight deviation compared to experimental results with the increase of packing fraction. This can be possibly due to less number of collisions between simulated particles compare to experiments. This problem can be avoided in the future by random displacement of particles to new locations.

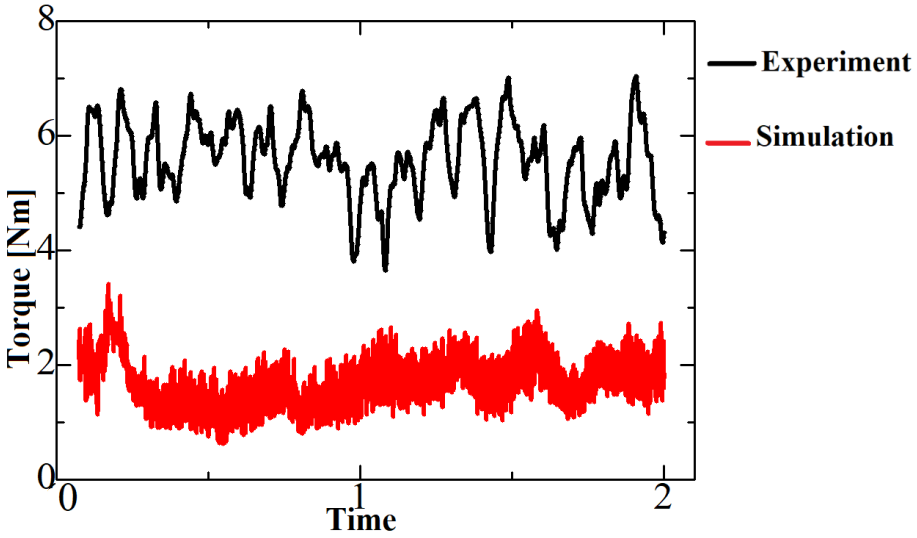

Fig.3.8 Time history of the typical damper torque, the packing fraction is 60% and the rotational speed is 60 rpm

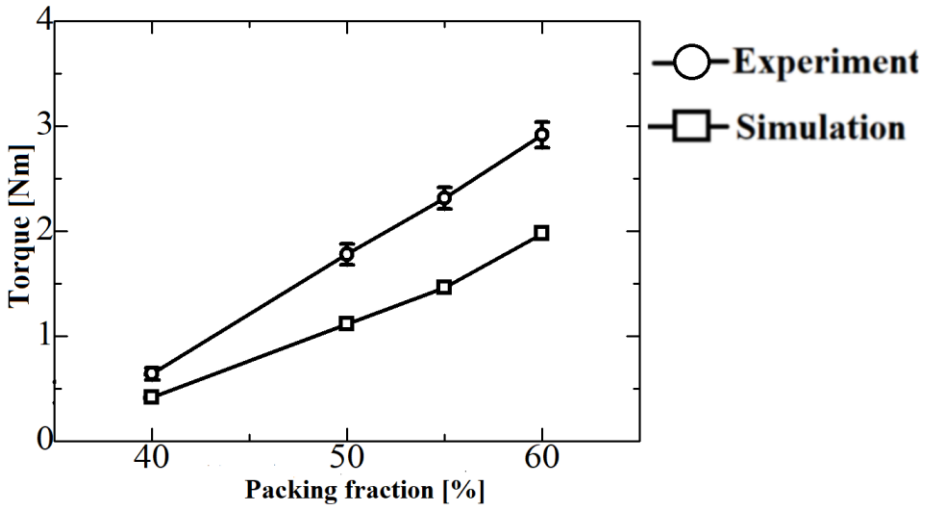

Fig.3.9 Experimental and simulation results of the torque versus packing fraction curve using elastomer particles of aspect ratio 1. The rotational speed is 60 rpm.

3.4.4 Effect of paking fraction and rotor speed on damper torque

Figure 3.10 shows the torque vs. packing fraction of the spherical elastomer particles (aspect ratio 1) and ellipsoidal elastomer particles (aspect ratio 1.2 and 1.5). Similar observations are made with elastomers of spherical and ellipsoidal particles; they both showed an increase of damper torque with the increase of packing fraction. The main reason is that number of particles decreases inside the damper with the

decrease of packing fraction [83]. In the particle dampers, the number of particles packed in the damper influences the damping behavior substantially. Even a small variation in particle number leads to a significant change in damping behavior. When the number of particles decreases, the volume of void space in the damper increases. At a low packing fraction, when the elastomer particles are pushed by the rotor, the particles move towards the void space. Due to void space, the particles do not apply strong frictional forces on each other and the walls of the damper [20]. However, when the void space is small, the particles are held by neighboring particles, so the elastomer particles' compression increases. The elastic deformation of particles plays a significant role in increasing the elastic repulsive force. When the void space inside the damper is small, the particles have strong elastic repulsive forces. To understand this phenomenon, we compare the cases of 30% and 50% packing fractions. In the case of 30% packing fraction, empty space exists inside the damper, while this space is very less in the case of 50% packing friction, as shown in Fig 3.11. At 30% packing fraction, when forces are applied on the particles by the rotor, the particle utilizes the available space inside the damper and move toward empty space; that is, in the case of 30% packing fraction, weak compression force acts on the particles.

From Fig. 3.10, the damper torque increases not only because of the packing fraction but also the rotational speed of the rotor. One of the main reasons is that the forces acting on the particles are not strong enough at low rotation speed because elastomer particles utilize the void space inside the damper and move towards the voaid space. At high rotation speed, the particles do not have enough time delay to move toward the available voaid space inside the damper. The second reason is the increase in the number of impacts between particles-particle and particle-wall at the high rotation speed of the rotor. A high-speed rotor pushes the elastomer particles with higher velocity, and particles impact with other particles, and transfer of energy occurs between

particle-particle and particle-wall.

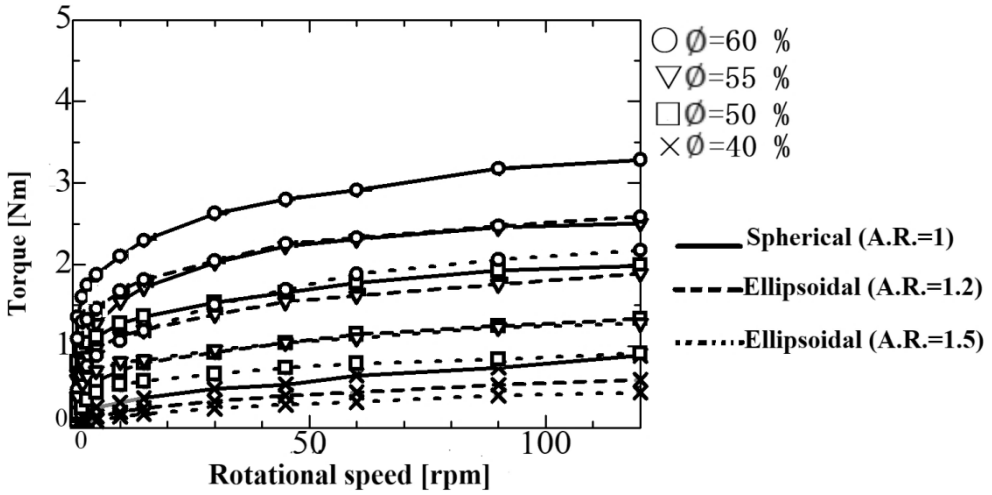

Fig.3.10 The torque versus rotor speed curve using particles with aspect ratio (A.R.) of 1, 1.2 and 1.5.

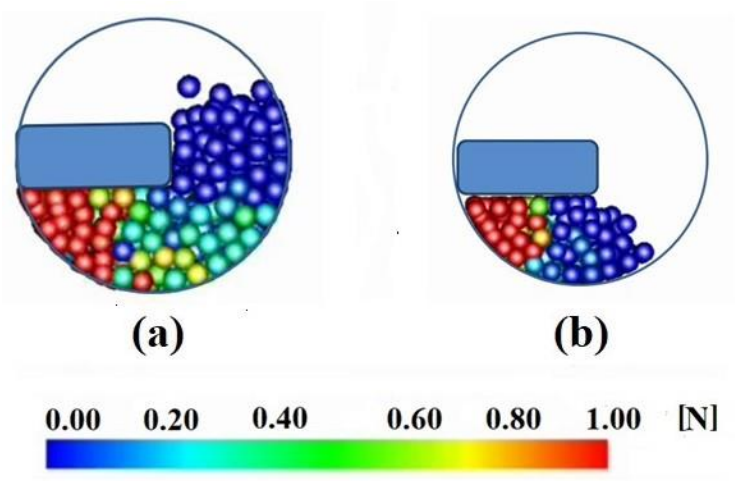

Fig.3.11 (a) more number of particles under compression 50% packing fraction, (b) Less number of particles under compression at 30% packing fraction.

3.4.5 Effect of shape of elastomer particles on damper torque

Figure 3.12 shows the damper torque and aspect ratio graph by varying the packing fraction at a rotor speed of 120 rpm. As the aspect ratio increases, the damper torque decreases. Spherical elastomer particles can produce higher damper torque compare to ellipsoidal elastomer particles. In the case of spherical particles, rotational motion is dominant, resulting in low shear resistance [86]. An increase in aspect ratio increases

the interlocking, which decreases the rotation tendency [87]. As a consequence, ellipsoidal particles slide over each with strong frictional shear resistance [88]. Due to the strong shear forces of ellipsoidal particles, the collisions and rotation between particle-particle and particle-wall decreases. To produce higher damper torque, particle rotation and particle translation is dominant factor [89-91]. For samples made of higher aspect ratio, rotation between particles becomes less significant [92, 93].

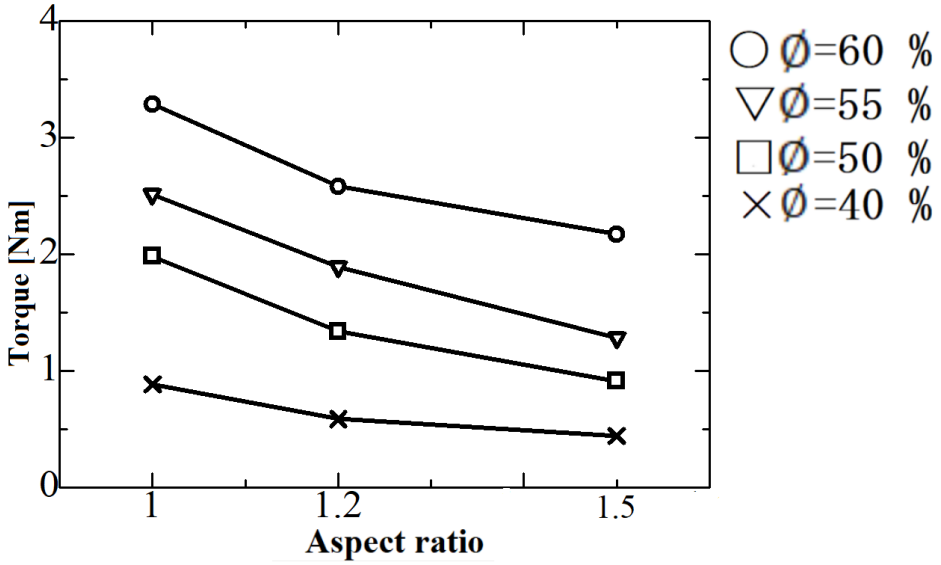

Fig.3.12 Torque versus aspect ratio curve at rotational speed of 120 rpm

3.4.6 Effect of mixing of spherical and ellipsoidal particles

Single-chamber rotary elastomer particle damper is used to investigate the effect of mixing spherical and ellipsoidal particles on damper torque. Figure 3.13 shows the experimental results of the mixture of spherical and ellipsoidal particles with 50:50 ratios. The graph shows that the spherical elastomers produce higher damper torque; however, the 60% packing fraction provideresults provide new insight into the analysis. The mixed mode was expected to provide higher damper torque due to combination of strong normal and shear forces. The mixed mode showed the expected results at 60% packing fraction because at 60%, the void gaps reduced due to an increase in the number of particles. At a low packing fraction, the gaps inside the damper are not letting particles apply strong normal and tangential contact forces at each other and walls of the damper. The maximum damper torque of mix mode at 60% packing fraction is 4.7 Nm,

which is observed at 45 rpm. The damper torque starts to decline after 45 rpm because the rotational motion of the particles decreases after 45 rpm. At high rpm, some of the particles in front of the rotor start to slide instead of rotating. Particle sliding decreases the rotational motion, and the number of collisions also decreases [94-95]. Particle sliding may produce a dense cluster region inside the damper, which decreases the damper torque after 45 rpm. We can expect to derive the strong damper torque by mixing spherical and ellipsoidal particles when the packing fraction is high. In the near future, the damping torque at higher packing fraction with mixing ratios of 60:40, 70:30, and vice versa should be investigated.

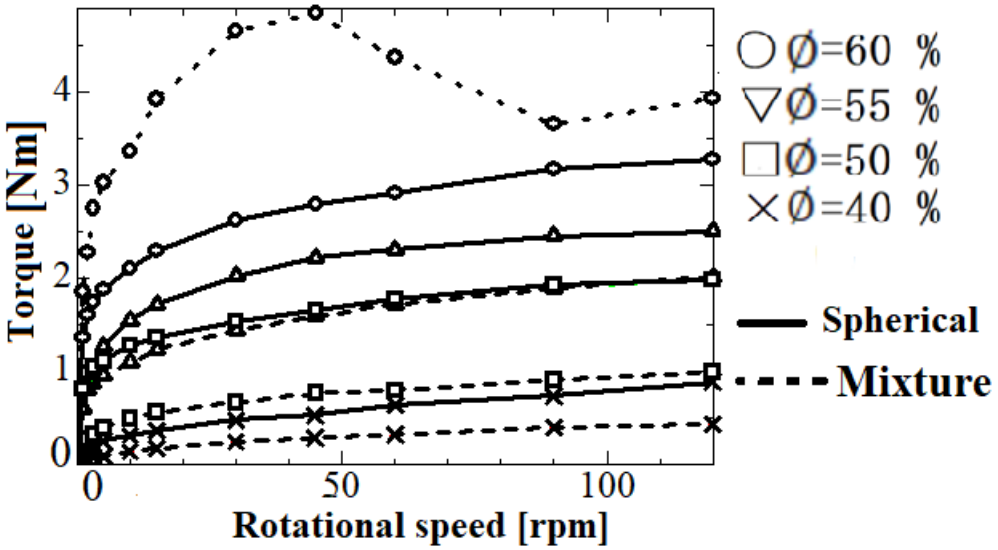

Fig.3.13 The torque versus rotor speed curve using a mixture of spherical and ellipsoidal particles.

3.4.7 Effect of type of elastomer particles on damper torque

Effect of type of elastomer particles on damper torque was investigated.The single-chamber rotary elastomer particle damper is used to investigate the effect of the type of elastomer particles. Elastomer particles made from TSE3466 and TSE3453 were used inside the damper as a damping medium. Figure 3.14 shows the torque vs. rotational speed curve of particles made from TSE3466 and TSE3453. In the graphs, the dotted lines represent the test results of particles made from TSE3453, and solid lines represent the results of the particle made from TSE3466. It is observed that particles made from material with higher tensile strength and hardness can produce higher damper torque than those made from materials with lower tensile strength and hardness [96, 97]. The tensile strength of TSE3466 is 7.4 MPa, and the hardness is 60, whereas

the tensile strength of TSE3453 is 6.4 MPa, and the hardness is 40. TSE3453 has low hardness, so the particles made of TSE3453 deformed extensively during compression, so these particles were unable to generate high resistive forces like particles made from TSE3466.

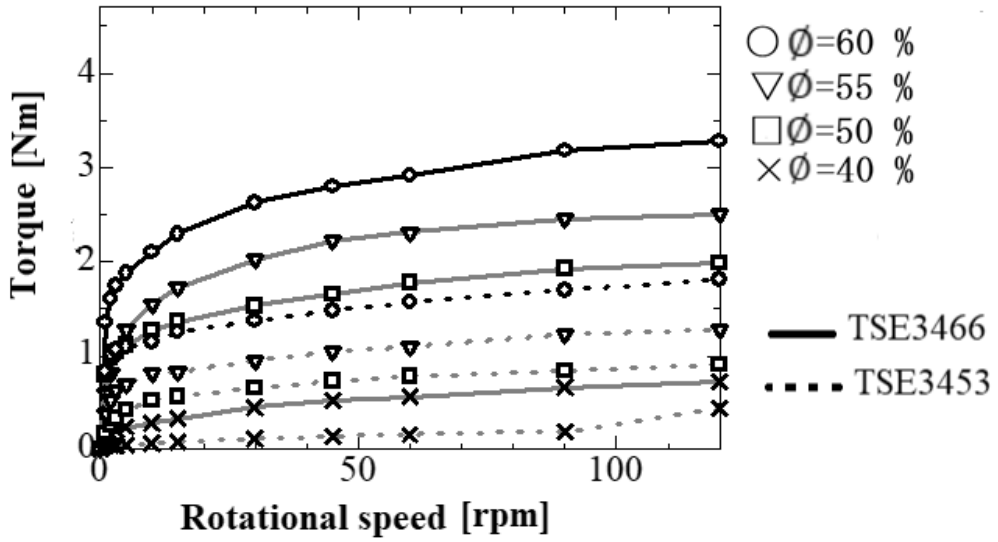

Fig.3.14 The torque versus rotor speed curve using particles made from TSE3466 and TSE3453 with aspect ratio 1.

3.5 Conclusion

The single-chamber rotary elastomer particle damper was prototyped and experimentally analyzed. Torque characteristics of the single-chamber rotary damper were studied with different packing fraction, rotor speed, type of elastomer materials, and aspect ratio of elastomer particles. The DEM simulation was conducted to investigate the behavior of spherical particles, while the behavior of the ellipsoidal particle was investigated by the visualization experiments. Increase of the packing fraction and the rotor speed increases the damper torque. Increase in aspect ratio of particles decreases the damper torque. The damper torque characteristics can be controlled by changing not only the packing fraction but also the aspect ratio of the ellipsoidal elastomer particles. Mixing of spherical and ellipsoidal particles at 50:50 ratios in rotary particle damper at 60% packing fraction increases the damper torque. Elastomer particles made of materials with higher tensile strength and hardness can produce higher damper torque.

4. Rotary Elastomer Particle Damper, the Effect of Gap and No-gap between Rotor and Cylinder

4.1 Introduction

Several factors can affect the damping performance of particle dampers, such as packing fraction and size of particles. However, due to the change in these parameters, there was a massive change observed in damping properties of damper because these changes can cause a change in the cooperative moment of damping particles. The gap between the rotor and cylinder can also significantly change the cooperative moment of particles inside the damper. The performance of a particle damper is affected by the packing fraction and size of particles. None of the studies examined the role of the gap between the rotor and the cylinder in a rotary elastomer particle damper. So it is essential to do an in-depth study on the behavior of elastomer particles considering the effect of the gap between the rotor and cylinder, which can affect the damping capabilities of a rotary elastomer particle damper. This research provides new insight into the research on particle dampers. In addition, the findings of this research can help academia and industry to design more efficient rotors for particle damper applications. This section proposes rotary elastomer particle dampers with gap and no gap between rotor and cylinder.

It is expected that the rotary elastomer particle damper with the gap between rotor and cylinder can provide a strong damper torque than the rotary elastomer particle damper with no gap between rotor and cylinder. Rotary elastomer particles damper with no gap model produces torque due to resistance of particles due to friction and collision between particle-particle and particle-wall of the damper but in case of rotary elastomer particle damper with gap model, extra layers of strongly compressed elastomer particles can enter the gap between the rotor and the body. Because of the elastic properties of the elastomer particles, the particles in the gap region can provide high repulsive forces in the motion of the rotor. The shear deformation is an important factor in ensuring high damping of the particle damper having gap between rotor and cylinder. When the particles are small in size and cross through the gap between rotor and cylinder without going through shear deformation, which is not beneficial for achieving a high damper torque. However, the large size particles of can go through high shear deformation while crossing the gap between rotor and cylinder thus, there is a direct co-relation between

repulsive forces from the particles and damper torque.

In this chapter the damper torque characteristics of rotary elastomer particle damper having the gaps between the rotor and damper body were investigated. The effects of packing fraction, rotor speed and size of elastomer particles on damper torque were examined. The behavior of elastomer particles inside the damper were analyzed by numerical simulations using the DEM.

4.2 Experimental procedure

4.2.1 Rotary damper with gap and no-gap between rotar and cylinder

The schematic diagram of the damper used in this experiment is shown in Fig. 4.1; the damper consisted of the body, cover, rotor, holder, shaft, and bearings. All dimensions in the figure are in millimeters (mm). In this damper, the holder's job was to hold the damper while performing experiments; it stopped the damper body from rotation. There were two tapered roller bearings (NTN30202) used in the damper, which supported the rotor of the rotary damper with gap damper. The parts other than the bearings were made of stainless steel SAE304. The damper was tested with no particles inside, and it produced quite small damping torque, so it can be stated that bearings and damper parts do not affect the test results. Due to the gap between the rotor and cylinder, an extra layer of elastomer particle can create a high frictional region on both sides of the rotor. The main reason behind selecting this damper is its simple working mechanism, which helped to understand and answer the article's primary research question. This damper size is suitable for several mechanical engineering applications, i.e., car seat suspension or automobile door closer. In the future, the prototype can easily be tested for practical application due to its small size.

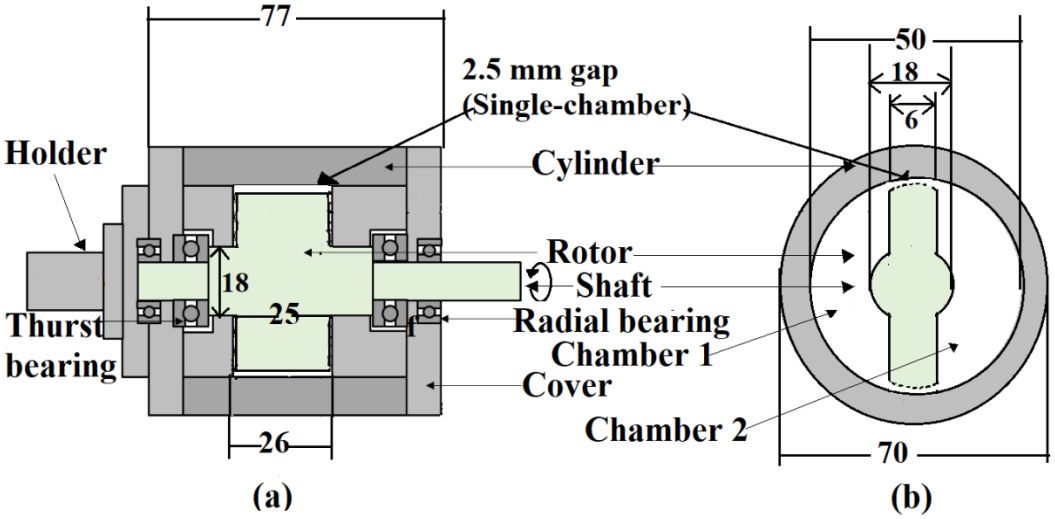

Fig.4.1 Schematic diagram of the damper with gap between rotar and cylinder. (a) Cross-sectional side view and (b) cross-sectional top view.

4.2.2 Working mechanism of the damper with gap between rotar and cylinder

The working mechanism of the damper is simple. As the shaft of the damper moved, the rotor attached to the shaft also started to move. As the rotor moved, it forces the elastomer particles to move in the direction of the rotor. The rotor pushes elastomer particles to move forward. Elastomers generate resistive forces in the motion of the rotor. These resistive forces are elastic forces, frictional forces, and viscous forces. These forces act between particle to particle and particle to wall of the damper. Due to the influence of these resistive forces, the damper generates a damping torque. The working mechanism of the damper with the gap between rotor and cylinder is different from the double-chamber rotary elastomer particle damper. The damper with the gap between rotor and cylinder particles can from one section of the damper to the other section. Particles that enter the gap between the rotor and cylinder can go through an enormous compression phase, resulting in a strong friction region inside the damper. The gap between rotor and cylinder can cause an increased stresses due to strong shear deformation of particles. Large size particles due to large contact area and large deformation capability can go through strong shear deformation.

4.3 Results and discussion

4.3.1 Torque generation mechanism of rotary damper with gap and no-gap between rotar and cylinder

We have performed extensive experiments to analyze the damper torque performance of rotary elastomer particle dampers. The qualitative and quantitative analysis of the rotary damper is also performed via numerical simulation. The purpose of the simulation is to allow us to analyze the behavior of the elastomer particles inside the damper. We first present simulation and experiment results to study the behavior of particles, followed by a detailed analysis of the damper torque properties using rotary elastomer particle damper with gap and no-gap model prototypes. Figures 4.2 and 4.3 show the torque versus time graph of the gap and no-gap models of the rotary elastomer particle damper. Figures 4.2 and 4.3 show the simulation results and the experimental results of rotary elastomer particle damper at 60 rpm and 50% packing fraction using particles of 3 mm diameter. To investigate the effect of particle deformation and particle sliding, decomposition of both the factors based on simulation results is conducted. The decomposition results are taken from 50% packing fraction at 60 rpm, using 3 mm diameter elastomer particles. From Fig. 4.4, the torque due to particle deformation is higher than the torque due to sliding friction. The dominant source of torque generation is particle deformation, so the compression force on particles plays a significant role in producing higher damper torque. Particles under higher compressive forces tend to generate strong repulsive forces in the rotation of the rotor. Due to repulsive forces from the particles, damper torque is produced by the damper.

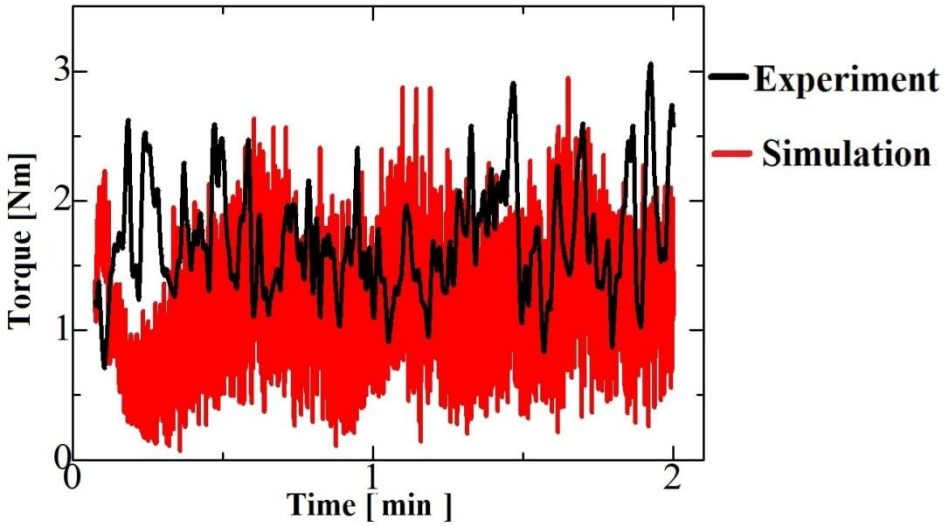

Fig.4.2 Time history of the rotary damper with gap model using 3 mm diameter particles, the packing fraction is 50% and the rotational speed is 60 rpm

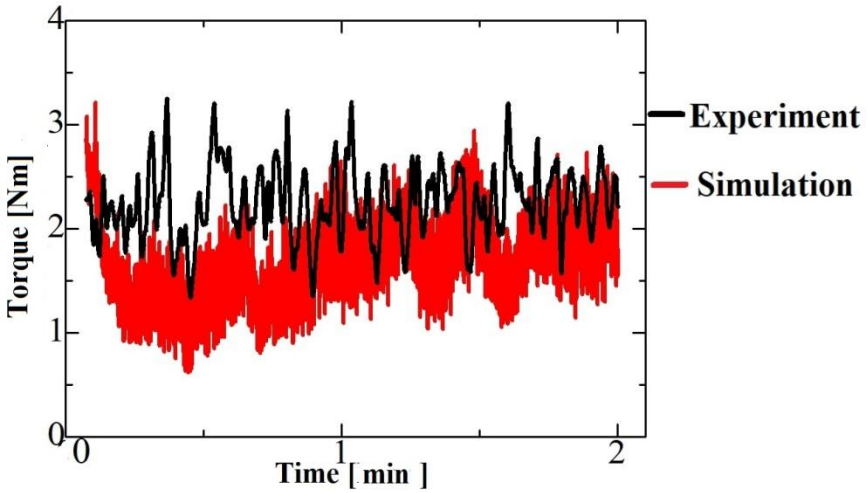

Fig.4.3 Time history of the rotary damper with no-gap model using 3 mm diameter particles, the packing fraction 50% is and the rotational speed is 60 rpm

Figure 4.5 shows the experimental and simulation results of the torque versus packing fraction curve using elastomer particles of 3 mm diameter in the no-gap model. The results are taken from the rotational speed of 60 rpm. From Fig. 4.5, the simulation results are in good agreement with experimental results. The experimental curve shows slightly higher torque than simulation results; this may be because of the surface roughness factor of the particles, which is not considered in the simulation. In our future research, this difference between experimental and simulation results can be reduced by considering the effect of the surface roughness factor in simulations. However, the

accuracy of DEM simulation has been largely overlooked due to the lack of suitable stochastic DEM data. DEM simulation can fill the needs currently but high-accuracy open access DEM can also be produced.We therefore encourage scientists to embrace particle damping simulation using DEM ensembles and try to increase the accuracy by collaboration with DEM vendors and scientists alike.

The design with gap and no gap between rotor and cylinder produced no audible noise is generated experiments. Due to the elastic nature of elastomer particles, they deform on collision and compression but no audible noise is generated. Due to the collision between elastomer particles, the sound is inaudible to humans, but it may be possible to record or measure it using a microphone. Figures 4.6 and 4.7 show the qualitative results obtained from the rotary elastomer particle damper simulation with no gap and gap models. To investigate the force of compression on the elastomer particles, the simulations were conducted at 50% packing fraction at the rotational speed of 60 rpm, using 3 mm diameter elastomer particles.

From Figs. 4.6 and 4.7, the strength of compressive force on the particles depends on the rotor's location inside the cylinder. When the rotor rotates, it forces the elastomer particles to move forward in the direction of the rotor rotation. Particles in front of the rotor push other particles to move forward. The force of compression on the elastomer particles is investigated using simulation results. From Figs. 4.6 and 4.7, several particles have a strong force of compression near the rotor, due to a strong repulsive force from the elastomer particles. When the rotor is at the bottom area of the cylinder, the force of compression is strong because the gravitational force is also acting on the particles. The elastic repulsive force of particles is produced by the collision of elastomer particles and frictional forces between particle-particle and particle-wall.

It is important to mention that the rotary damper with the gap between rotor and cylinder and no-gap between rotor and cylinder may look similar, but in the case of the gap model, due to the gap between the damper body and the rotor, an extra layer of elastomer particles are formed. In the gap between rotor and cylinder, particles are under a strongly compressed state. The shear deformation rate of elastomer particles is high while passing through the gap between rotor and cylinder. Due to strong shear deformation of elastomer particles in the gap region a strong friction zone inside the

damper is produced.

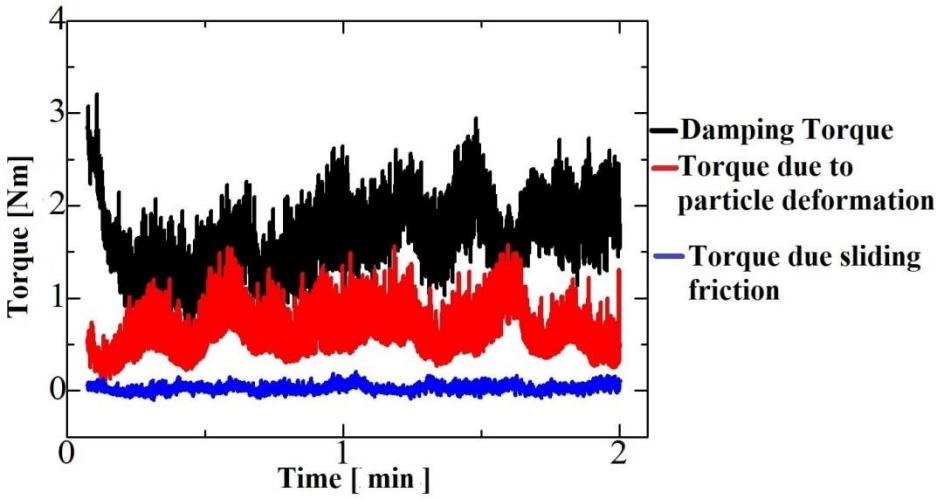

Fig.4.4 Time history of the rotary damper with no-gap model using 3 mm diameter particles, decomposition of torque due to particle deformation and torque due to sliding friction

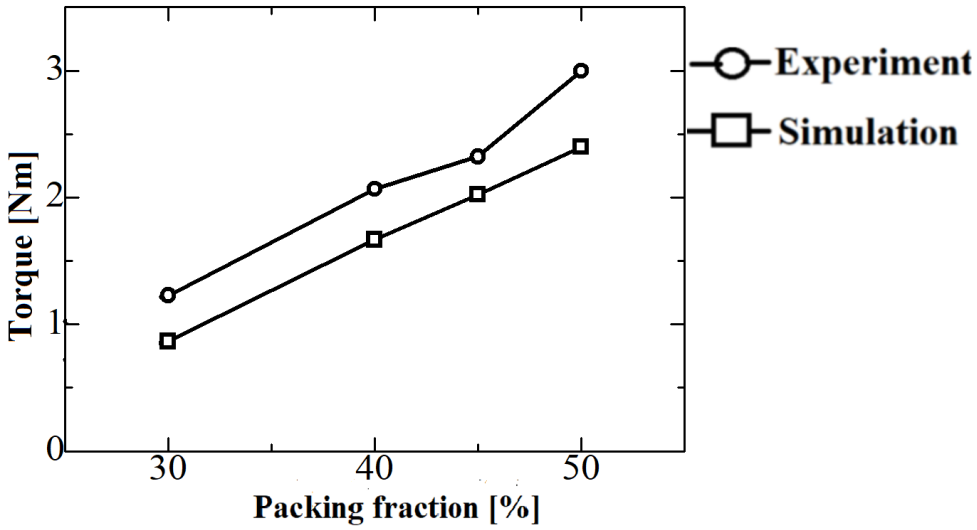

Fig.4.5 Experimental and simulation results of the torque versus packing fraction curve using elastomer particles of 3 mm diameter in no-gap model. The rotational speed is 60 rpm.

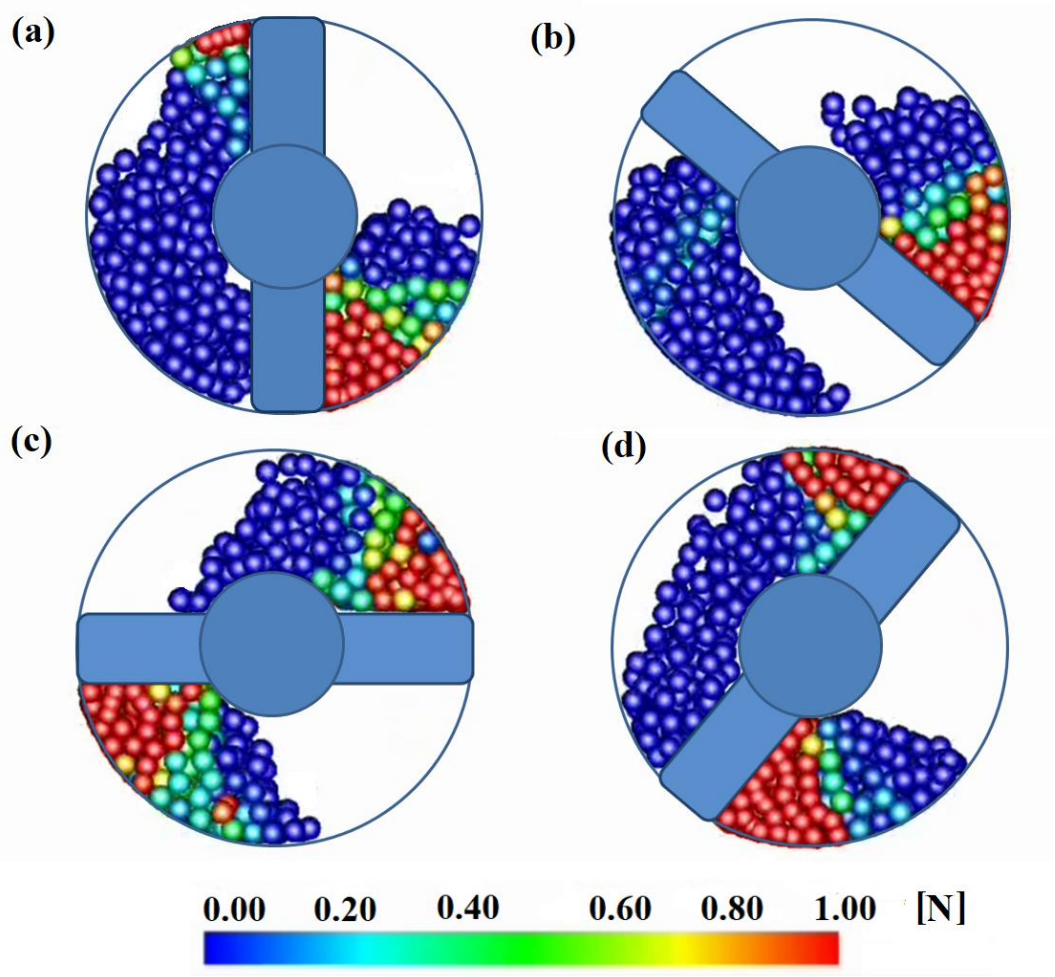

Fig.4.6 Compressive force acting on the particle inside the rotary damper with no-gap model, packing fraction 50% and the rotational speed of 60 rpm (a) 0 degree, (b) 45 degree, (c) 90 degree, (d) 135 degree. The direction of rotation is counter-clockwise

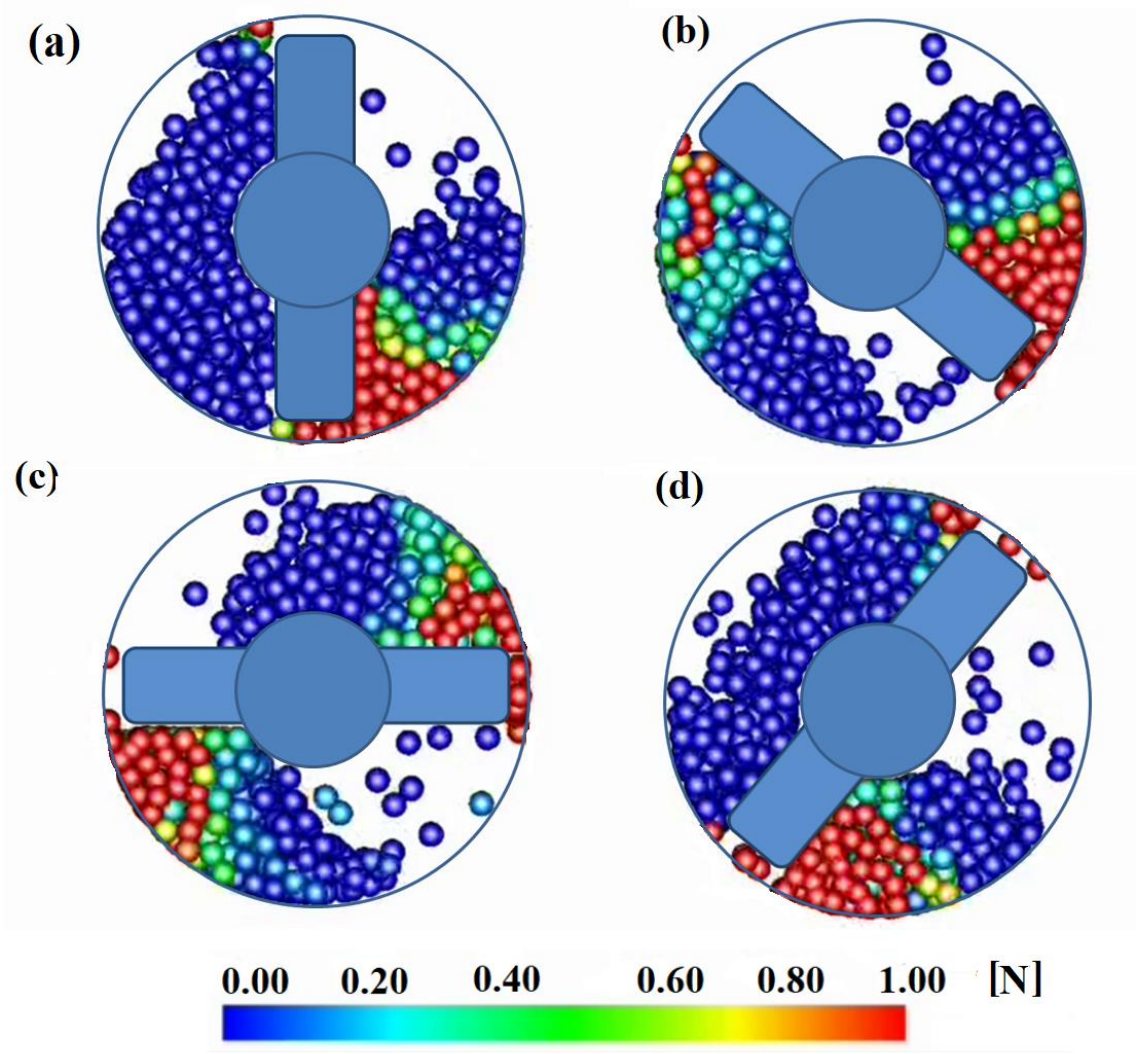

Fig.4.7 Compressive force acting on the particle inside the rotary damper with gap model, packing fraction 50% and the rotational speed of 60 rpm (a) 0 degree, (b) 45 degree, (c) 90 degree, (d) 135 degree. The direction of rotation is counter-clockwise

4.3.2 Effect of paking fraction and rotor speed on gap and no-gap rotary elatomer particle damper

Rotary elastomer particle dampers with gap and no-gap show an increase in damper torque with the increase of packing fraction. Figure 4.8 shows the torque vs. packing fraction graph of the no-gap model of the rotary elastomer particle damper. Figure 4.9 shows the torque vs. packing fraction graph of the gap model of rotary elastomer particle dampers. Similar observations are made in gap and no-gap models of rotary elastomer particle dampers; they both showed an increase in damper torque with the increase of packing fraction. The main reason is that the number of particles

decreases inside the damper with a decrease in packing fraction [97]. A small variation in particle number leads to a large change in damping behavior. A decrease in the number of particles increases the volume of void space in the rotary elastomer particle damper. When elastomer particles are moved forward by the rotor at a high packing fraction, the particles do not have void spaces available.

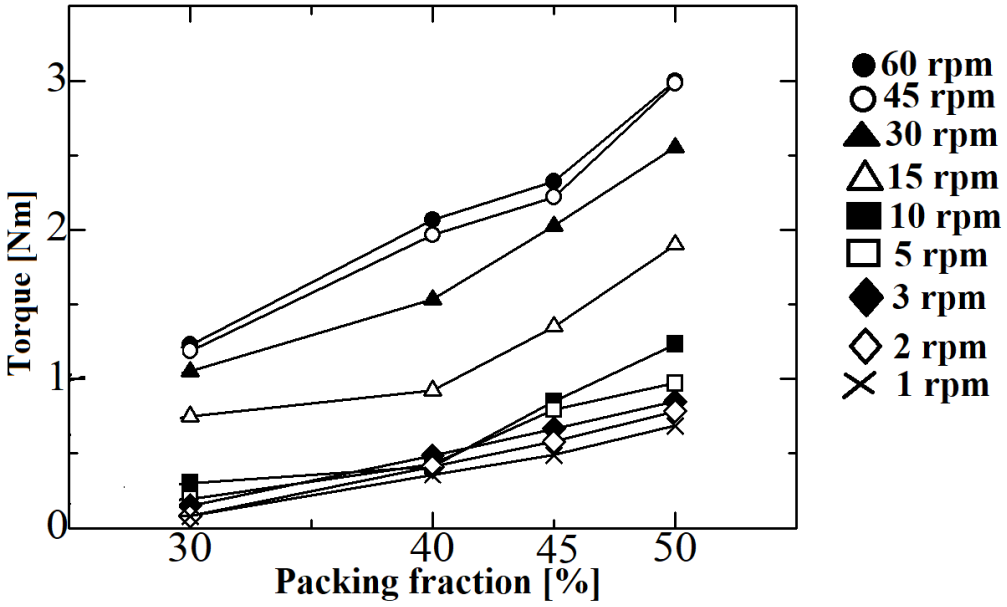

Fig.4.8 The torque versus packing fraction curve of rotary damper with no-gap between rotor and cylinder, using 3 mm diameter particle made from TSE3466

When there is void space, particles do not apply strong frictional forces on each other and the walls of the damper [98, 99]. However, when the void space is large, the particles are not strongly compressed by neighboring particles, so particles produce weak repulsive forces. The elastic deformation of elastomer particles inside the damper plays a vital role in increasing the damper torque. In short, when there are less void spaces inside the damper, particles can produce strong damper torque. As illustrated in Figs. 4.8 and 4.9, the damper torque increases not only because of the packing fraction but also the rotational speed of the rotor. One of the important factors which cause an increase in damper torque with the increase of rotor speed is the normal and tangential forces acting on the elastomer particles are strong at the high speed of the rotor. The

second reason is the increase in the number of collisions between particles-particle and particle-wall. A high-speed rotor pushes the elastomer particles with higher velocity, and particles collide with neighboring particles with high velocity, and loss of energy takes place. From Fig.4.9, at low rotation speed upto 10 rpmsof the shaft, the damper torque of rotary damper with the gap between rotor and cylinder is higher than the rotary damper with no-gap between rotor and cylinder. At rotation speed higher than 10 rpm of the shaft, the rotary elastomer damper with no-gap model has higher damper torque than the rotary damper with gap model using 3 mm diameter particles. From 1 to 10 rpm the gap-model produced higher damper torque because particles are crossing the gap region by rolling motion at low speed of rotor. At the high rpm of the shaft, the particle's rolling motion is converted to sliding motion [100] when passing through the gap region. In conclusion, due to sliding motion at high rpm, compressive force on particles reduced; that is why, the no-gap model's damper torque is higher than the rotary damper with gap model at rotation speed higher than 10 rpm.

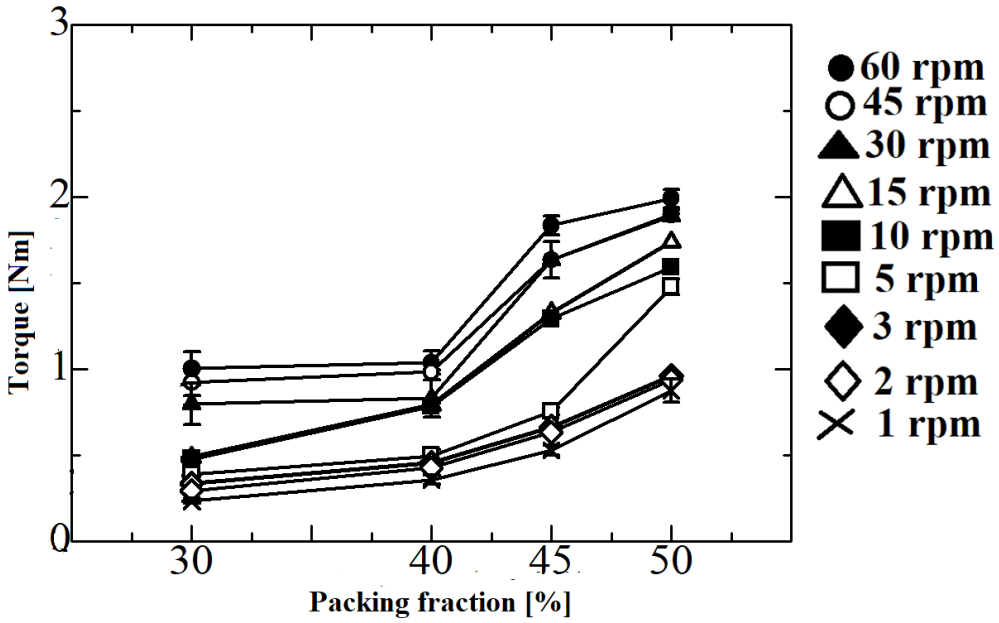

Fig.4.9 The torque versus packing fraction curve of rotary damper with gap between rotor and cylinder, using 3 mm diameter particle made from TSE3466

It is worth mentioning that an increase in packing fraction and the rotational speed increases the damper torque, however, it has certain limitations. At high rotational speed such as 100 and 120 rpm, breaking rate of the particle is higher. Similarly, high rpm of

the rotor for a long period can also break the particles.

Previous studies [3, 37 and 85] showed that, when the packing fraction is higher than certain value, decline in the damping is observed in metallic particle dampers, while in the case of elastomer damper at the packing fraction up to 50%, the damper torque kept increasing. We could not observe the limit of packing fraction which the damper torque may reduce in rotary elastomer particle damper because; it is difficult to close the cylinder at high packing fractions such as 70% and above.

4.3.3 Effect of size of elastomer particles on damper with gap between rotor and cylinder

The particles of 3 mm, 4 mm, and 5 mm made from TSE3466 were experimentally tested. This section of the study demonstrates a correlation between the damper torque and the size of elastomer particles. Although the mass ratio is kept constant, the number of particles would vary. In the case of the gap and no-gap model increase in damper, torque is observed with the increase of the size of the elastomer parties.

Figure 4.10 shows the collective results of 3 mm, 4 mm, and 5 mm diameter particles at 60 rpm. It is observed that the size of elastomer particles plays a significant role in increasing the damper torque of a rotary elastomer particle damper. A significant increase in damper torque is obtained when 5 mm diameter elastomer particles are used. The main reason behind the increase in the damper torque with the increase in particle size is the higher deformation capability in large-sized particles. Due to collision and friction between particles and damper body, the velocity of the adjacent particles drops. Particle velocity drops when two particles collide with each other and compress each other. The greater energy dissipation and damping take place when collision and compression are transferred to neighboring particles. Large particles have more contact area and can deform more than small particles under a compressed state. In brief, large size particles tend to produce strong repulsive forces so resulting in strong damper torque. It is worth mentioning that when 5 mm diameter particles are used inside the rotary damper with gap mode, it produces higher damper torque than the rotary damper with the no-gap model.

When the particles of 5 mm diameter enter into the gap, the particles were under

intense compressive force due to larger deformation capability. In summary, unlike 3 mm and 4 mm diameter particles, 5 mm particles are in a strongly compressed state even at high rpm, resulting in a strong damper torque generation.

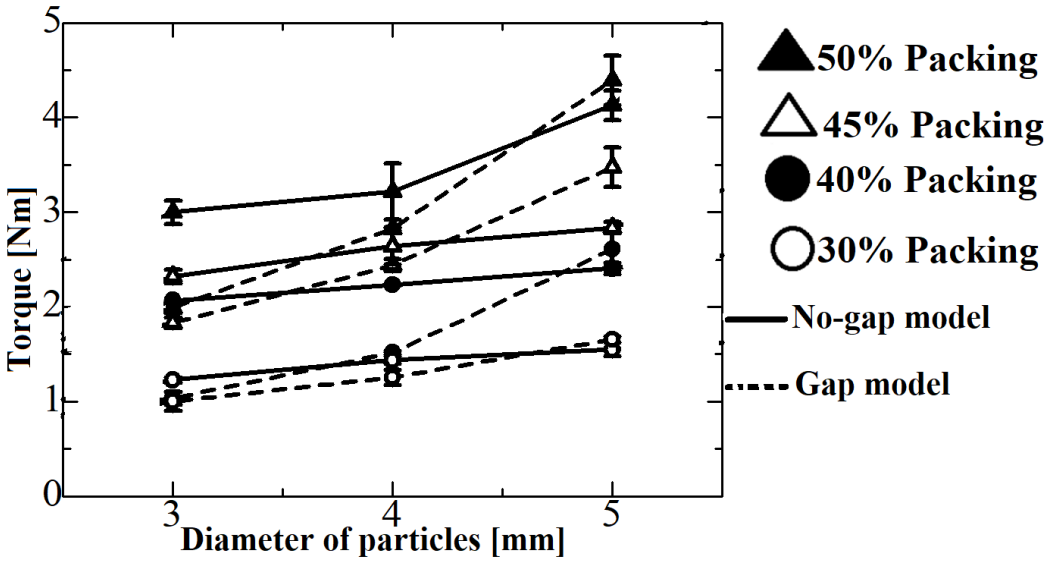

Fig.4.10 The torque versus diameter of the particle curve of rotary damper with gap and no-gap models at 60 rpm

4.3.4 Effect of gap between rotor and cylinder

As illustrated in Fig.4.11, damper torque of rotary damper with gap model using 3 mm diameter particles is higher than no-gap model at the rotataion speed up to 10 rpm. At the low rotation of the shaft, particles slowly cross through the gap region, while easily rotating through the gap. This rotation of particles turns into a sliding motion when the rotor strongly pushes particles at high rotation speed (more than 10 rpm). In summary, particles do not go through enormous compression at high rotation speed while crossing through the gap region. At high rotation speed, they quickly cross the gap region by sliding, which results in weak compressive forces on the particles. However, in the case of the rotary damper with the no-gap model, the neighboring particles support particles in front of the rotor. In the gap model, the particles cross from the gap region, so at high rotation speed, the neighboring particle's support is weak compare to the rotary damper with no-gap.

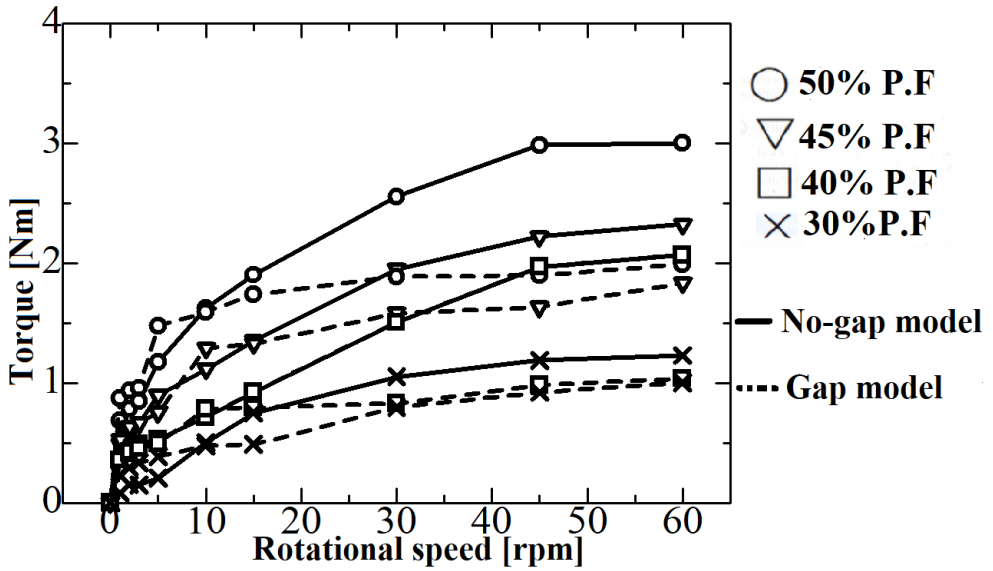

Fig.4.11 The torque versus rotational speed curve of rotary damper with gap and no-gap using 3 mm diameter elastomer particles

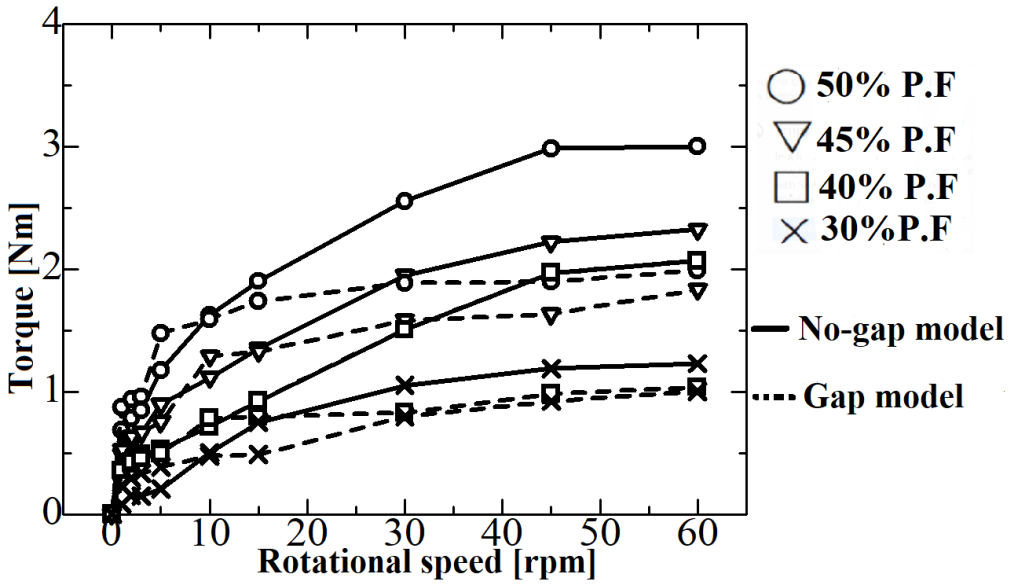

Fig.4.12 The torque versus rotational speed curve of rotary damper with gap and no-gap models using 5 mm diameter elastomer particles

From Fig.4.12, interesting results were obtained when elastomer particles of 5 mm diameter are used. The damper torque of the rotary damper with the gap model is larger than the rotary damper with the no-gap model when 5 mm diameter particles are used. Because of the higher deformation capability of 5 mm diameter particles compare to 4 mm and 3 mm diameter particles. 5 mm diameter particles have more contact area, and

they can deform more under a compressed state. In conclusion, 5 mm diameter elastomer particles tend to produce strong repulsive forces, resulting in strong damper torque. In summary, unlike 3 mm and 4 mm diameter particles, 5 mm particles are in the strongly compressed state even at high rotation speed, resulting in a strong damper torque generation.

4.4 Conclusion

We investigated the effect of change in packing fraction, rotor speed and size of elastomer particles on the damper torque. Prototypes of the rotary elastomer particles damper with gap and no-gap between rotor and cylinder were prepared to observe the damper torque performance of rotary elastomer damper. Spherical elastomer particles made from TSE3466 were tested in the rotary damper with 3 mm, 4 mm, and 5 mm diameters. An increase in damper torque is observed by increasing the packing fraction. Particles made of TSE3466 were tested to observe the effect of the particles' size on damper performance. It is proved that 5 mm diameter particles showed higher damper torque than 4 mm and 3 mm diameter particles. Interestingly, the damper torque of the rotary damper with the gap model was higher than the no-gap model at rotation speed upto 10 rpm when 3 mm diameter elastomer particles are used. The damper torque of the rotary damper with the gap between rotor and cylinder is larger than that of the rotary damper with no-gap model throughout any rotation speeds when 5 mm diameter elastomer particles are used.

5. Conclusion and Future Works

5.1 Conclusion

The vibration control is considered a key element in mechanical engineering to ensure the safety and comfort of the users of the mechanical engineering systems. To decrease the vibration of any mechanical setup, an effective vibration control system is necessary. In conventional dampers, viscoelastic materials and viscous oils are used to control the vibration. One of the main problems with conventional dampers is that the performance is sensitive to the temperature. In a rotor-based particle damper a rotating shaft is used inside the damper. In research, the damper torque characteristics of rotary elastomer particle damper were investigated. The effects of packing fraction, rotor speed size of elastomer particles, types of elastomer particles and aspect ratio of particles on the damper torque of rotary elastomer particle damper were examined. To understand the behavior of particles inside the damper, the numerical simulations using the discrete element method and visualization experiment were performed. An experimental setup is used to investigate damper torque characteristics of rotary elastomer particle damper.

In rotor-based particle dampers, some particles are under strong compressive stress, and some are weakly compressed. From the simulation analysis in chapters 2, 3, and 4, it can be stated that particles in front of the rotor are strongly compressed than the particles far from the rotor. The particles that are away from the rotor support the particles which are in front of the rotor. The particles in the high compressive zone (in front of the rotor) contribute more in the generation of damper torque than particles in the less compressive zone. The particles in front of the rotor have limited motion between the particles due to strong compressive forces. Particles far from the rotor contribute in the generation of damper torque by collision with each other and the wall of the damper. An increase in the aspect ratio of particles decreases the damper torque. The damper torque characteristics can be controlled by changing not only the packing fraction but also the aspect ratio of the ellipsoidal elastomer particles. Mixing of spherical and ellipsoidal particles at 50:50 ratios in rotary particle damper at 60% packing fraction increases the damper torque. Particles made of materials with high

tensile strength and hardness produced strong damper torque than particles made of materials with low tensile strength and hardness. An increase in the size of the particles increases the damper torque. It is experimentally shown that 5 mm diameter particles produced higher damper torque than 4 mm and 3 mm diameter particles. The damper torque of the rotary damper with the gap model was higher than the no-gap model at rotation speed upto 10 rpm when 3 mm diameter elastomer particles are used. The damper torque of the rotary damper with the gap between rotor and cylinder is larger than that of the rotary damper with no-gap model throughout any rotation speeds when 5 mm diameter elastomer particles are used.

Gravity also plays an important role in increasing the damper torque. The effect of gravity varies according to the angle of the rotor. At 90 degree and 180 degree angles of double-chamber rotary damper the compressive force of the particles becomes higher due to gravitational force. The gravitational force generates resistive forces in the particle's motion, and particles apply strong repulsive forces on the rotor. At 270 degree angle of the rotor, particles drop from top to bottom on the left side of the damper. Gravity attracts the elastomer particles pushes them away from the rotor, so the weak compression forces is developed at rotor angle 270 degrees. The compressive force is stronger at 0 degree angle of the rotor, because at 0 degree; the gravity is acting on the particles in downward direction. Gravity holds the particles which incrases the frictional force. The effect of gravity some times reduces the damper torque. Effect of gravity can be over comed by installing the angle at different angles.

5.2 Recommendations for future research

In this dissertation some shortcomings were identified that need further investigation. In the rest of this section, a number of future recommended tasks are listed below.

The scope of this research was restricted by the capabilities of the experimental setup used in this study. The torque measuring range of the torque meter is limited so size of particles was restricted to some limitations. Updating the expriemntal setup will enable us to test particle dampers over a wider operating range and expand the current research to more generalised environment.

An investigation of different shapes of particles can be conducted. This will enable a closer look at the effect of the shape of particles on performance in general.

Simulation of ellipsoidal elastomer particles can help to understand the behavior of ellipsoidal particles inside the damper. DEM software dedicated for particle behavior simulation in which numerical models of different particle shapes can be investigated; this will be a great benefit to research in the field of particle damping. One of the main problems in general for DEM simulations is its long calculation time. Upgrading GPU systems can shorten the calculation time. DEM simulation model to investigate the behavior of semi-active rotary particle damper can also be one of the important challenges for future research.

Acknowledgements

First of all, I would like to thank Allah, God the Almighty, the Most Merciful, and the Most Beneficial. I wish to thank Prof. Yasushi Ido, my Ph.D. supervisor, for his motivation and guidance during my graduate study. I am lucky to have such a decent and nicest professor ever. I wish to thank Dr. Yuhiro Iwamoto for giving me his valuable time and advice.

This thesis has been improved from the original version and reviewed before presenting at the thesis defense. I am thankful to my lead supervisor and other professors for giving valuable advice to improve my thesis. I was awarded a scholarship from The Ministry of Education, Culture, Sports, Science, and Technology (MEXT), which supported me during my Ph.D. I am thankful to my supervisor, MEXT, and Nagoya Institute of Technology International student office for their support. I must also acknowledge Dr. Atsushi Toyouchi, Mr. Kishan, Mr. Obata, and Mr. Kosaka for their suggestions and for giving me the basic knowledge about DEM simulations. I also thank my best friend Muhammad Asad for motivating me during my hard time. He helped to make my time in the Ph.D. program more fun and interesting. Needless to say, this entire exercise would be at most a dream if it was not for my loving family. To my parents, Atta Muhammad Golo and Akhtiaran Khatoon, education has been as important as breathing in life, and my father has always encouraged me for my studies and gave me the freedom to select any career I want.

Nomenclature

a radius of the particle [mm]
C_n viscosity coefficient in a normal direction
C_t viscosity coefficient in the tangential direction
E_i moduli of longitudinal elasticity of the particle
E_w moduli of longitudinal elasticity of the particle-wall
$\boldsymbol{F}_{cn}$ normal contact force [N]
$\boldsymbol{F}_{ct}$ force in tangential direction [N]
$\boldsymbol{F}_g$ gravity force
$\boldsymbol{F}_i$ sum of forces [N]
$\boldsymbol{g}$ gravitational acceleration vector [m/s^2]
G_i transverse elastic modulus of the particle
I_i moment of inertia [kg m^2]
K_n elastic modulus in normal direction
K_t elastic modulus in the tangential direction
K_{nij} elastic coefficient particles when the particle-wall contact
m_i mass of the particle [kg]
$\acute{c}_n$ combined roughness of two surfaces
β contact radius of smooth surfaces
$\boldsymbol{n}_i$ unit vector in the normal direction
λ surface roughness paramter
$\boldsymbol{r}_i$ position vector of the particle
t time [s]
$\boldsymbol{T}_i$ total torque [Nm]
$\boldsymbol{V}_{\hat{f}ij}$ tangential relative velocity [m/s]
$\boldsymbol{V}_{ij}$ relative velocity vector [m/s]
α magnitude of viscous damper force
$\boldsymbol{\Omega}_i$ angular velocity vector [rad/s]
ρ particle density [kg/m^3]
δ_n strain in the normal direction
δ_t strain in tangential direction
$\boldsymbol{\omega}_i$ angular velocity vectors of particles i
δ_{ct} displacement of particle in tangential direction
ν_i Poisson's ratios of the particle
ν_w Poisson's ratios of the wall
$\emptyset$ Packing fraction

References

[1] Housner, G. W, Bergman, L. A, Caughey, T. K and Masri, S. F: Structural Control: Past, Present, and Future, *Journal of Engineering Mechanics-asce,* **123** (1997), 897-971.

[2] Rakhio A., Dong X., Liu W.: Design and Testing of a Novel Vane Type Magnetorheological Damper. *Recent Advances in Intelligent Manufacturing*. *ICSEE*, **923** (2018), 257-266

[3] Friend, R. D. and Kinra, V. K.: Particle impact damping, *Journal of Sound and Vibration*, **233**-1 (2000), 93–118.

[4] Hollkamp, J. J. and Robert, W. G.: Experiments with particle damping, *Proc. 12th International Conference on smart structures and materials* (1998), 2–12.

[5] Flint, E. M.: Experimental measurements of the particle damping effectiveness under centrifugal loads, *Proc. 4th International Conference National Turbine Engine High Cycle Fatigue* (1999), 1–6.

[6] Xiao, W., Jaiani, L., Sheng, W. and Fang, X.: Study on vibration suppression based on particle damping in centrifugal field of gear transmission, *Journal of Sound and Vibration*, **366**-1 (2015), 62-80.

[7] Xu, Z., Wang, M. Y., Chenc, T.: Particle damper for vibration and noise reduction, J*ournal of Sound and Vibration*, **270** (2004), 1033-1040.

[8] Yan, W., Jun, W. and Chen, Y.: Experimental Research on the Effects of a Tuned Particle Damper on a Viaduct System under Seismic Loads, *Journal of Bridge Engineering*, **19**-3 (2014), 3304-3316.

[9] Lenggana, B.W.; Ubaidillah, U.; Imaduddin, F.; Choi, S.-B.; Purwana, Y.M.; Harjana, H. Review of Magnetorheological Damping Systems on a Seismic Building. *Applied Science*, **11** (2021), 9339.

[10] Morishita, Y., Ido, Y., Maekawa, K. and Toyouchi, A.: Basic Damping Property of a Double-Rod Type Damper Utilizing an Elastomer Particle Assemblage, *Advanced Experimental Mechanics*, **1** (2016), 93-98.

[11] Liu, W., Tomlinson, G. R. and Rongong, J. A.: The dynamic characterization of disk geometry particle dampers, *Journal of Sound and Vibration*, **280**-3 (2005), 849-861.

[12] Marhadi, S. F. and Kinra, V. K.: Particle impact damping: effect of mass ratio, material, and shape, *Journal of Sound and Vibration*, **286**-2 (2005), 433-448.

[13] Panossian, H.V.: Structural Damping Enhancement Via Non-Obstructive Particle Damping

Technique, *The Journal of Vibration and Acoustics*, **114**-1 (1991), 101-105.

[14] Paget, A. L.: Vibration in steam turbine buckets and damping by impacts, *Engineering* **143**, (1937), 305-307.

[15] Lieber, P. and Jensen, D.: An acceleration damper: Development, design and some applications. *Trans. ASME* , **67** (1945), 523–530.

[16] Lu, Z., Masri, S. F. and Lu, X.: Studies of the performance of particle dampers attached to a two-degrees-of-freedom system under random excitation, *Journal of Vibration and Control*, **17** (2011), 1454-1471.

[17] Araki, Y., Yokomichi, I.: Impact Dampers With Granular Materials, *JSME*, **28** (1985), 1466–1472.

[18] Saeki, M.: Analytical study of multi-particle damping, *Journal of Sound and Vibration*, **281** (2015), 1133-1144.

[19] Masri, S. F.: Analytical and Experimental Studies of Multiple‐Unit Impact Dampers, *Journal of the Acoustical Society of America*, **45**, (1969) 1111-1117.

[20] Hang, Y., Wang, Y., Liu, B. and Jiang, X.: Experimental Study on the Damping Effect of Multi-Unit Particle Dampers Applied to Bracket Structure, *Applied Sciences.* **9,** (2019) 2912.

[21] Panossian, H. V.: Structural Damping Enhancement Via Non-Obstructive Particle Damping Technique, *Journal of Vibration and Acoustics*, **114**-1 (1991), 101-105.

[22] Hayashi, K., and Ido, Y.: Damper damping characteristics using the fluidity of granules, *Journal of the Japanese Society for Experimental mechanics*, **10** (2010), 63-68 (in Japanese).

[23] Ido, Y., Hanai, M., Kawai, T., Hayashi, K. and Toyouchi, A.: Effects of container size, stroke and frequency on damping properties of a damper using a steel particle assemblage, *Advanced Experimental Mechanics*, **1** (2016), 105-110.

[24] Hanai, M., Ido, Y., Iwamoto, Y., Nishizawa, T., Hayashi, K., Discrete Element Method Simulation of Dynamic Behavior of Particles in a Damper Using a Steel Particle Assemblage, *Asian Conference on Experimental Mechanics*, (2016), 352-353.

[25] Kawamoto, R., Ido, Y. and Hayashi, K.: Influence of installation angle of a damper using a magnetic particle assemblage on damping force under applied magnetic field, *Journal of the Japan Society of Applied Electromagnetics and Mechanics*, **23** (2015), 624-629.

[26] Binoy, M., Shah, Jeremy J. Nudell, Kevin R. Kao, Leon M. Keer, Q. Jane Wang, Kun Zhou.: Semi-active particle-based damping systems controlled by magnetic fields, *Journal of Sound*

and Vibration, **330**, (2011), 182-193.

[27] Gharib, M. and Ghani, S.: Free vibration analysis of linear particle chain impact damper, *Journal of Sound and Vibration*, **332**, (2013), 6254-6264.

[28] Kawamoto, R., Ido, Y. and Toyouchi, A.: Damping Properties of a Damper Using an Elastomer Particle Assemblage Containing Fine Particles, *Advanced Experimental Mechanics*, **1** (2016), 99-104.

[29] Toyouchi, A., Hanai, M., Ido, Y. and Iwamoto, Y.: Damper force characteristics of a separated dual-chamber single-rod-type damper using an elastomer-particle assemblage, *Journal of Sound and Vibration*, **488** (2020), 115625.

[30] Kishan, K. K., Ido, Y., Iwamoto, Y. and Toyouchi, A.: Experimental Investigation of Angle Dependent Torque Properties of a Particle Rotary Damper Using a Magnetic Elastomer Particle Assemblage, *International Symposium on Applied Electromagnetics and Mechanics*, **64** (2020), 737-743

[31] Li, K. N. & Darby. A.: A buffered impact damper for multi‐degree‐of‐freedom structural control. *Earthquake Engineering & Structural Dynamics*, **37** (2008), 1491 - 1510.

[32] Du, Y. and Wang, S.: Modeling the fine particle impact damper, *International Journal of Mechanical Sciences*, **52** (2010), 1015-1022.

[33] Darabi, B. and Rongong, J. A.: Polymeric particle dampers under steady-state vertical vibrations. *Journal of Sound and Vibration*, **331**(2012), 3304–3316.

[34] Bustamante, M., Gerges, S., Cordioli, J., Martin, O., Weisbeck, J. and Ott, M.: Experimental study on some parameters that affect the performance of an elastomer particle damper, *Proceedings of Meetings on Acoustic*, (2013) 19. 10.1121/1.4801066.

[35] Michon, G., Ahmad, A. and Gwenaëlle, A.: Soft Hollow Particle Damping Identification in Honeycomb Structures, *Journal of Sound and Vibration*, **332** (2013), 536–544.

[36] Hamzeh, P., Parteli, E. and Pöschel, T.: Granular dampers: Does particle shape matter?, *Journal of Physics*, **18**-7 (2016), 73-82.

[37] Kachare, P.S, and Bimlesh, K.: Effect of particle size and packing ratio of PID on vibration amplitude of beam, *Journal of Mechanical Engineering and Sciences*, **4**-1 (2013), 504-517.

[38] Kerwin, E. M.: Macromechanisms of Damping in Composite Structures, in Internal Friction, Damping, and Cyclic Plasticity, ed. B. Lazan (West Conshohocken, PA: ASTM International, 1965), 125-149.

[39] Popplewell, N. and Semercigil, S.E.: Performance of the bean bag impact damper for a sinusoidal external force, *Journal of Sound and Vibration*, **133** (1989), 193-223.

[40] Wong, C. X., Daniel, M. C. and Rongong, J. A.: Energy dissipation prediction of particle

dampers, *Journal of Sound and Vibration*, **319** (2009), 91-118.

[41] Zhang, K., Chen, T., Wang, X. and Fang, J.: Rheology behavior and optimal damping effect of granular particles in a non-obstructive particle damper, *Journal of Sound and Vibration*, **364**, (2016), 30-43.

[42] Snchez, M., Rosenthal, G. and Pugnaloni, L. A.: Universal response of optimal granular damping devices, *Journal of Sound Vibration*, **331** (2012), 4389–4394.

[43] Snchez, M., Carlevaro, M. A. and Pugnaloni, L. A.: Effect of particle shape and fragmentation on the response of particle dampers, *J. Vib. Control*, **20** (2014), 1846–1854.

[44] Cundall, P.A. A Computer Model for Simulating Progressive Large Scale Movements in Blocky Rock Systems. Proceedings of the Symposium of the International Society for Rock Mechanics, *Society for Rock Mechanics* (ISRM), France, II-8 (1971).

[45] Zhou, Xian-Qi., Xu, W.-Y., Niu, X.-Q and Cui, Y.-Z.: Review of distinct element method researching progress and application, *Yantu Lixue/Rock and Soil Mechanics*, **28** (2007), 408-416.

[46] Lu, Z., Chen, X., Zhang, D. and Dai, K.: Experimental and analytical study on the performance of particle tuned mass dampers under seismic excitation, *International association of earthquick engineering*, **46** (2016), 697-714.

[47] Sanchez, M., and Carlevaro, M. A.: Nonlinear dynamic analysis of an optimal particle damper. *Journal of Sound and Vibration* **332** (2013), 2070-2080.

[48] Attia, M. and Waterhouse, R.: Standardization of Fretting Fa-tigue Test Methods and Equipment, ASTM international pub-lishing company, (1992) West Conshohocken, Philadelphia Pa, USA.

[49] Ji, Q., Kuan-Ching, Li., Hai, J., Qingguo, Z. and Lei, Y.: GPU-accelerated DEM implementation with CUDA, *International Journal of Computational Science and Engineering*, **330** (2015), 330-337

[50] Du, Y., and Zhenxing, G.: Research on a New Particle Impact Damper. *IOP Conference Series: Materials Science and Engineering*, **381** (2018), 012073.

[51] Daniel, E.: Damping of Rotating Beams with Particle Dampers: Discrete Element Method Analysis. *AIP Conference Proceedings*, **1542** (2013), 867-870.

[52] Zhang, Y., Xu, W., Zhang, Y. and Qian, F.: Comparative study of the damping performance of concentrated masses and particle dampers based on cantilever beams, *AIP Advances*, **11** (2021) 105319.

[53] Li, X., Yang, Y. and Shi, W.: Study on the Damping Effect of Particle Dampers considering Different

Surface Properties, *Shock and Vibration*, **2019** (2019), 8293654.

[54] Hollkamp, J. and Gordon, R. W.: Experiments with particle damping, *Proceedings, Smart Structures and Materials*, **3327** (1998).

[55] Senthilkumar, M., Mohanasundaram, K. M. and Sathishkumar K.: Impact of Particle Damping Parameters on Surface Roughness of Bored Surface. *Arabian Journal for Science and Engineering*, **39** (2014), 7327-7334.

[56] Louis, G., Marco, M. and Gian, G.: A review of particle damping modeling and testing. *Journal of Sound and Vibration*, **459** (2019), 114865.

[57] Xiao, W., Shao, W., Shi, J., Luo, Y., Wang, S.; Effect of particle restitution coefficient on high-power gear transmission with dynamic continuum and non-continuum coupling, *Journal of Advanced Mechanical Design, Systems, and Manufacturing*, **15** (2021), JAMDSM0033-JAMDSM0033.

[58] Żurawski, M. and Zalewski, R.: Damping of Beam Vibrations Using Tuned Particles Impact Damper. *Applied Sciences*, **10** (2020), 6334.

[59] Brouwers, H. J.: Particle-size distribution and packing fraction of geometric random packings, *Physica Review. E*, **74** (2011) 031309.

[60] Mutabaruka, P., Taiebat, M. and Radjai, F.: Effects of size polydispersity on random close-packed configurations of spherical particles, *Physical Review E*, **100, (**2019), 042906.

[61] Simon, D. R.: Sound absorption by suspensions of nonspherical particles: Measurements compared with predictions using various particle sizing techniques, *Journal of the Acoustical Society of America*, **114** (2003) 1841-1850.

[62] Lu, Z., Wang, Z., Masri, S. F., and Lu, X.: Particle impact dampers: Past, present, and future. *Structural Control and Health Monitoring*, **25** (2018), e2058.

[63] Song, L., Xiao, W., Guo, H., Yang, Z., and Li, Z.: Particle damping applied research on mining dump truck vibration control. *AIP Conference Proceedings*, **1967** (2018), 030039.

[64] Haseena, A.: A structural vibration using solid particle damper, *Journal of Engineering Research and Applications*, **5** (2015), 01-09.

[65] Yang, Y. and Yu, Y.: Design and Simulation of Long Slender end Mill Embedded with Passive Damper, *Procedia Engineering* , **99** (2015), 1380 -1384.

[66] Du, Y., Wang, S., Zhu, Y., Li, L., and Han, G.: Performance of a new fine particle impact damper, *Advances in Acoustics and Vibration*, **2008** (2008), 140894.

[67] Marhadi, K. S., & Kinra, V. K.: Particle impact damping: effect of mass ratio, material, and shape. *Journal of sound and vibration*, **283** (2005), 433-448.

[68] Xu, Z., Wang, M. and Chen, T.: A Particle Damper For Vibration and Noise Reduction, *Journal of Sound and Vibration*, **270** (2004), 1033-1040.

[69] Zhaowang, X., Xiandong, L. and Yingchun, S.: Application of particle damping for vibration attenuation in brake drum, *International Journal of Vehicle Noise and Vibration*, **7** (2011), 178 - 194.

[70] Zhang, Z. L., Chen, J. B. and Li, J.: Theoretical study and experimental verification of vibration control of offshore wind turbines by a ball vibration absorber, *Structure and Infrastructure Engineering*, **10** (2014), 1087.

[71] Jin, J., Yang, W., Hyo-In, K and Junhong, P.: Development of tuned particle impact damper for reduction of transient railway vibrations, *Applied Acoustics*, **169** (2020), 107487.

[72] Papalou, A. and Strepelias, E.: Effectiveness of particle dampers in reducing monuments' response under dynamic loads, *Mechanics of Advanced Materials and Structures*, **23** (2016), 128-135.

[73] Ido, Y., Hayashi, K. and Kawai,T.: Damping force of a semiactive damper utilizing magnetic particles under applied magnetic field, *International Journal of Applied Electromagnetics and Mechanics*, **39** (2012), 535-540.

[74] Meyer, N. and Seifried, R.: Toward a design methodology for particle dampers by analyzing their energy dissipation. *Computationa Paricle Mechics*, **8** (2021), 681–699.

[75] Ono, N., Kitamura, K., Nakajima, K. and Shimanuk, Y.: Measurement of Young's Modulus of Silicon Single Crystal at High Temperature and Its Dependency on Boron Concentration Using the Flexural Vibration Method, *Japanese Journal of Applied Physics*, **39**-1 **(**2000), 368-371.

[76] Catherine, S.: Particle-Based Discrete Element Modeling: Geomechanics Perspective, *International Journal of Geomechanics*, **11**-6 (2011), 449-464.

[77] Cundall, P. A., and Strack, O. D. L.: A Discrete Numerical Model for Granular Assemblies, *Geotechnique*, **29**-1 (1979), 47-65.

[78] Sunday, C., Murdoch, N., Tardivel, S. and Stephen, R., Michel, P.: Validating N-body code Chrono for granular DEM simulations in reduced-gravity environments, *Monthly Notices of the Royal Astronomical Society*, **498**-1 (2020), 1062-1079.

[79] Sakai, M.: How Should the Discrete Element Method Be Applied in Industrial Systems?: A Review, *KONA Powder and Particle Journal*, **33**-1 (2016), 169-178.

[80] Mindlin, R. D.: Compliance of elastic bodies in contact, *Transaction of ASME, Series E, Journal of Applied Mechanics*,**16** (1949), 259–268.

[81] The Japan Society of Mechanical Engineers, JSME mechanical engineers' handbook, 6 ed. (1977), **3**-34, Maruzen Publishing Co.,Ltd. (in Japanese)

[82] Mittal, K., Dutta, S. and Fischer, P.: Direct Numerical Simulation of Rotating Ellipsoidal Particles

using Moving Nonconforming Schwarz-Spectral Element Method, *Computers & Fluids*, **205** (2020), 104556.

[83] Alireza, K. and Zahra, M.: Influence of non-spherical shape approximation on DEM simulation accuracy by multi-sphere method, *Powder Technology*, **332** (2018), 265-278.

[84] Yeom, S., Ha, E., Kim, M., Jeong, S. H., Hwang. S., Choi, D. H.: Application of the Discrete Element Method for Manufacturing Process Simulation in the Pharmaceutical Industry, *Pharmaceutics*, **11**(2019), 414.

[85] Papalou, A. and Masri, S. F.: Response of Impact Dampers with Granular Materials Under Random Excitation, Earthquake Engineering and Structural Dynamics, **25**-3 (1996), 253-267.

[86] Ting, J. and Corkum, B.: Strength behavior of granular materials using discrete numerical modeling, , Ting, J. and B. Corkum.: Strength behavior of granular materials using discrete numerical modelling, *International conference on numerical methods in geomechanics*, **6** (1988), 305-310.

[87] Ting, J., Meachum, L. Aand Rowell, J.: Effect of particle shape on the strength and deformation mechanism of ellipse shape granular assemblies, *Engineering Computations*, **12** (1995), 99-108.

[88] John, F., Abbaspour-Fard., Kremmer, M., Raji, A. O.: Shape representation of axi-symmetrical, non-spherical particles in discrete element simulation using multi-element model particles, *Engineering Computations*, **16** (1999) 467-480.

[89] Shakeel, M., Hamid, A., Atta, U., John, M. and Ryoichi, Y.: Direct Numerical Simulations of Correlated Settling Particles, *Journal of the Physical Society of Japan*, **87** (2018), 064402.

[90] Eric J. R. P.: DEM simulation of particles of complex shapes using the multisphere method: Application for additive manufacturing, *AIP Conference Proceedings* **1542**, (2013) 185-188.

[91] Hossain, M., Zhu, H. P. and Yu, A. B.: Numerical investigation on effect of particle aspect ratio on the dynamical behaviour of ellipsoidal particle flow, *Journal of Physics: Condensed Matter,* **33** (2021), 455102.

[92] Xie, Y., Yang, Z. and Daniel, B.: The Influence of Particles' Aspect Ratio on the Shear Behaviour of Granular Materials, *International Conference on Discrete Element Methods*, **188** (2017), 253-264.

[93] Zhai, C., Herbold, E. B., Hall, S.A., Hurley, R. C.:Particle rotations and energy dissipation during mechanical compression of granular materials, *Journal of the Mechanics and Physics of Solids*, **129** (2019), 19-38.

[94] Takahashi, Y. and Sekine, M.: Examination of Particle Behavior in Container on Multi-Particle Collision Damper, *Machines*, **3** (2015), 242-255.

[95] Kamal, C., Gravelle, S., & Botto, L.: Effect of hydrodynamic slip on the rotational dynamics of a thin Brownian platelet in shear flow. *Journal of Fluid Mechanics,* **919** (2021), A1.

[96] Mao, K., Wang, M. Y., Xu, Z., and Chen, T.: Simulation and Characterization of Particle Damping in Transient Vibrations, ASME. *J. Vib. Acoust*, **126** (2004), 202–211.

[97] Lawrance, G., Varadarajan, A.and Sam, P.: Effect of material on damping characteristics of impact mass during hard turning, *Emerging Materials Research.* **4** (2015), 81-88.

[98] Eric, P., Jochen, S., Christina, B., Karl-Ernst, W., Wolfgang, P. and Thorsten, P.: Attractive particle interaction forces and packing density of fine glass powders, *Scientific reports*, **4** (2014) 6227.

[99] Shilong, L and Jiong, T.: On Vibration Suppression and Energy Dissipation Using Tuned Mass Particle Damper, *Journal of Vibration and Acoustics*, **139** (2016), 4034777.

[100] Davidson, J., Scott, D., Bird, P., Herbert, O., Powell, A., Ramsay, H.: Granular Motion in a Rotary Kiln: the Transition from Avalanching to Rolling, *KONA Powder and Particle Journal*, **18** (2000), 149-156.

List of Publications

1. Rakhio, A., Ido, Y. and Iwamoto, Y, Toyouchi, A.: Experimental Analysis of Rotary Damper: Effect of Using Spherical and Ellipsoidal Elastomer Particles on Damping, *Advanced Experimental Mechanics*, 6 (2021), 90-97.
2. Rakhio, A., Ido, Y. and Iwamoto, Y, Toyouchi, A.: Experimental and Numerical Analyses of Torque Properties of a Separated Double-Chamber Rotary Damper Using Elastomer Particles, *Advanced Experimental Mechanics*, 6 (2021), 83-89.
3. Rakhio, A., Ido, Y. and Iwamoto, Y, Toyouchi, A.: Experimental and Numerical Analyses of Torque Properties of Rotary Elastomer Particle Damper Considering the Effect of Gap and No Gap between Rotor and Body of the Damper, *Shock and Vibration*, (2021), 7724156.
4. Allah Rakhio, Yasushi Ido, Yuhiro Iwamoto, Atsushi Toyouchi, Double-Chamber Rotary Elastomer Particle Damper: Does Particle Size Matters?, 16th International Symposium on Advanced Science and Technology in Experimental Mechanics, (Online) 2021.11.

International Confernces and Symposium

1. Allah Rakhio, Yasushi Ido, Yuhiro Iwamoto, Atsushi Toyouchi, Damper Torque of Semiactive Rotary Particle Damper Uisng Magnetic Particles under External Magnetic Field, 第 30 回 MAGDA コンファレンス (オンライン) 2021.12 日本 AEM 学会
2. Allah Rakhio, Yasushi Ido, Yuhiro Iwamoto, Atsushi Toyouchi, Double-Chamber Rotary Elastomer Particle Damper: Does Particle Size Matters?, 16th International Symposium on Advanced Science and Technology in Experimental Mechanics, (Online) 2021.11.
3. Allah Rakhio, Yasushi Ido, Yuhiro Iwamoto, Atsushi Toyouchi, Torque Properties of a rotary elastomer particle damper based on spherical and ellipsoidal elastomer particles, 18th International Conference on Flow Dynamics, (online) 2021.10.
4. Allah Rakhio, Yasushi Ido, Yuhiro Iwamoto, Atsushi Toyouchi, Rotrary Damper Using Elastomer Particles: Effect on Damping Torque due to Type of Elastomer Particles, BSSM's 15th International Conference on Advances in Experimental Mechanics, (Online) 2021.09.

5. Allah Rakhio, Yasushi Ido, Yuhiro Iwamoto, Atsushi Toyouchi, Double-Chamber Rotary Elastomer Particle Damper: Effect of the Size of the Elastomer Particles on the Torque, 日本実験力学会 2021 年度年次講演会　(オンライン)　2021.08.